UNIVERSIDADE DE SÃO PAULO
FACULDADE DE ZOOTECNIA E ENGENHARIA DE ALIMENTOS

ANNA CAROLINA MAZETO ERCOLIN

Caracterização tomográfica e ultrassonográfica de linfonodos normais, reativos e neoplásicos em cães

Pirassununga
2022

ANNA CAROLINA MAZETO ERCOLIN

Caracterização tomográfica e ultrassonográfica de linfonodos normais, reativos e neoplásicos em cães

Versão corrigida

Tese apresentada à Faculdade de Zootecnia e Engenharia de Alimentos da Universidade de São Paulo, como parte dos requisitos para a obtenção do título de Doutor em Ciências do programa de Pós-graduação em Biociência Animal.

Área de Concentração: Diagnóstico e Terapias Inovadoras

Orientador: Prof. Dr. Luciano Andrade Silva
Co-orientador: Prof. Dr. Robson Fortes Giglio

Pirassununga

2022

Ficha catalográfica elaborada pelo
Serviço de Biblioteca e Informação, FZEA/USP,
com os dados fornecidos pelo(a) autor(a)

Ercolin, Anna Carolina Mazeto
E65c Caracterização tomográfica e ultrassonográfica de linfonodos normais, reativos e neoplásicos em cães / Anna Carolina Mazeto Ercolin ; orientador Luciano Andrade Silva ; coorientador Robson Fortes Giglio. -- Pirassununga, 2022.
67 f.

Tese (Doutorado - Programa de Pós-Graduação em Biociência Animal) -- Faculdade de Zootecnia e Engenharia de Alimentos, Universidade de São Paulo.

1. Ultrassonografia. 2. Tomografia. 3. Linfonodo. 4. Cão. 5. Metástase. I. Silva, Luciano Andrade, orient. II. Giglio, Robson Fortes, coorient. III. Título.

UNIVERSIDADE DE SÃO PAULO
Faculdade de Zootecnia e Engenharia de Alimentos
Comitê de Ética em Pesquisa da FZEA

CERTIFICADO

Certificamos que a proposta intitulada "Características ultrassonográficas e tomográficas de linfonodos normais, reativos e neoplásicos em cães e sua correlação com citologia e histopatologia", protocolada sob o CEUA nº 9135150620 (ID 001510), sob a responsabilidade de **Anna Carolina Mazeto Ercolin** - que envolve a produção, manutenção e/ou utilização de animais pertencentes ao filo Chordata, subfilo Vertebrata (exceto o homem), para fins de pesquisa científica ou ensino - está de acordo com os preceitos da Lei 11.794 de 8 de outubro de 2008, com o Decreto 6.899 de 15 de julho de 2009, bem como com as normas editadas pelo Conselho Nacional de Controle da Experimentação Animal (CONCEA), e foi **aprovada** pela Comissão de Ética no Uso de Animais da Faculdade de Zootecnia e Engenharia de Alimentos da Universidade de São Paulo - FZEA/USP (CEUA/FZEA) na reunião de 02/07/2020.

We certify that the proposal "B-mode ultrasonographic and computed tomographic characteristics of normal, reactive, and neoplastic lymph nodes in dogs and their correlation to cytology and histopathology", utilizing 10 Dogs (males and females), protocol number CEUA 9135150620 (ID 001510), under the responsibility of **Anna Carolina Mazeto Ercolin** - which involves the production, maintenance and/or use of animals belonging to the phylum Chordata, subphylum Vertebrata (except human beings), for scientific research purposes or teaching - is in accordance with Law 11.794 of October 8, 2008, Decree 6899 of July 15, 2009, as well as with the rules issued by the National Council for Control of Animal Experimentation (CONCEA), and was **approved** by the Ethic Committee on Animal Use of the School of Animal Science and Food Engineering - (São Paulo University) (CEUA/FZEA) in the meeting of 07/02/2020.

Finalidade da Proposta: Pesquisa (Acadêmica)

Vigência da Proposta: de 01/2021 a 02/2021 Área: Biociência Animal

Origem:	Animais de proprietários						
Espécie:	Cães	sexo:	Machos e Fêmeas	idade:	1 a 5 anos	N:	10
Linhagem:	Inespecífico			Peso:	10 a 25 kg		

Local do experimento: O experimento será realizado na sala de ultrassonografia de pequenos animais da UDCH FZEA USP. Pirassununga, Sao Paulo, Brasil.

Pirassununga, 02 de julho de 2020

Profa. Dra. Cristiane Gonçalves Titto
Coordenadora da Comissão de Ética no Uso de Animais
Faculdade de Zootecnia e Engenharia de Alimentos da Universidade de São Paulo - FZEA/USP

Profa. Dra. Daniele dos Santos Martins
Vice-Coordenadora da Comissão de Ética no Uso de Animais
Faculdade de Zootecnia e Engenharia de Alimentos da Universidade de São Paulo - FZEA/USP

Para aquela que me ensinou que o verbo “desistir” não existe no dicionário, mãe, dedico.

Para aquele que foi a pessoa mais inteligente que eu já conheci, saudades eternas pai, dedico.

Para o meu anjo da guarda, meu porto seguro, meu raio de sol, Anna, dedico.

Para o meu melhor amigo, companheiro e amor, Ariel, dedico.

Para aquela que me ensinou a nadar independente das dificuldades,
Profa. Dra. Maria Cristina Ferrarini Nunes Soares Hage (*in memoriam*), dedico.

Agradecimentos

À Deus, fonte de toda a vida e sabedoria.

À todos os meus familiares por todo apoio e paciência.

Ao meu orientador, prof. Dr. Luciano Andrade Silva

Ao meu co-orientador, prof. Dr. Robson Fortes Giglio

À profa. Dra. Lilian Oliveira

À médica veterinária Luciane Kanayama

Ao Programa de Pós-Graduação em Biociência Animal, pela oportunidade de realização do curso de doutorado.

À Faculdade de Zootecnia e Engenharia de Alimentos, Departamento de Medicina Veterinária e Unidade Didático-Clínico Hospitalar, pelo apoio e infraestrutura oferecidos para a realização dessa pesquisa.

À University of Florida, pela infra-estrutura e material disponibilizado para a realização deste trabalho.

À Fundação de Amparo à Pesquisa do Estado de São Paulo pela concessão da bolsa de doutorado e pelo apoio financeiro para a realização desta pesquisa.

À CAPES pela concessão da bolsa de doutorado e pelo apoio financeiro para realização dessa pesquisa.

Às funcionárias da secretaria da pós-graduação Paula, Kefilin, Cecília, Érica pelo excelente trabalho e ajuda valiosa ao longo de todo o doutorado.

Às minhas amigas e colegas de pós-graduação do Setor de Imagem da UDCH FZEA USP, Camila, Tamiris, Sâmara, Amanda, Carolina, Raira, Camilla Schopp, Jessica Beraldo, Ana Paula

Às minhas amigas, que mesmo distante se fazem presente, Kadine, Cryskely, Anna Luiza, Jaqueline, Vívian, Daniela, Lillian, Kelly

Às minhas amigas, colegas de profissão e exemplos de profissionais, Juliana Casals, Filomena Denadai Fontana, Maira Carnielli e Andréia Santos Silva, meu respeito e minha admiração.

Ao Grupo de Oração Universitário Online da Diocese de Limeira.

À Dra. Lídia Maurino.

“Pois eu, o Senhor, teu Deus, eu te seguro pela mão, e te digo: “Nada temas, eu venho em teu auxílio… diz o Senhor, teu Redentor é o Santo de Israel.”
Isaías 41,13-15

RESUMO

ERCOLIN, A. C. M. ***Caracterização tomográfica e ultrassonográfica de linfonodos normais, reativos e neoplásicos em cães.*** 2022. 67 f. Tese (Doutorado) - Faculdade de Zootecnia e Engenharia de Alimentos, Universidade de São Paulo, Pirassununga, 2022.

Uma vasta gama de trabalhos científicos descrevem critérios ultrassonográficos e tomográficos que contribuem na diferenciação entre linfonodos normais e anormais, tanto na medicina como na veterinária. Contudo esses estudos descrevem linfonodos reativos e metastáticos no mesmo grupo e muitos não têm correlação com métodos de diagnóstico padrão ouro. O presente estudo investigou se processos inflamatórios e neoplásicos em linfonodos caninos produzem alterações anatomo-morfológicas suficientes para serem detectadas pela ultrassonografia e tomografia computadorizada. E ainda se as alterações detectadas nos exames de imagem são particulares para cada processo, permitindo a diferenciação entre linfonodos reativos e neoplásicos/metastáticos. A primeira etapa descreveu um estudo retrospectivo sobre a performance diagnóstica do ultrassom para classificação de linfonodos normais e linfadenopatias benignas e malignas. Foram avaliados 79 linfonodos craniais cervicais e 95 linfonodos inguinais e ilíaco mediais. A acurácia do ultrassom para diferenciação do *status* dos linfonodos variou com o tipo de linfonodo. Mais de 60% dos linfonodos com reforço acústico posterior formações císticas foram associados com malignidade. Na segunda etapa, uma revisão sistemática analisou evidências qualitativas para testar a hipótese de que a tomografia pode diferenciar linfonodos normais daqueles acometidos por processo inflamatório ou metastático. O padrão de realce de contraste heterogêneo e margens irregulares ou indistintas podem ser associados com etiologias malignas. A gordura perinodal é um meio de contraste natural que favorece a avaliação do linfonodo. Concluiu-se que ambas as modalidades de imagem se beneficiaram quando houve uma combinação de parâmetros, como por exemplo avaliação do "contorno e gordura perinodal" para tomografia e "tamanho e ecotextura" para ultrassonografia. Todavia, exames de citologia ou histopatologia são as técnicas padrão ouro para o diagnóstico de processos neoplásicos ou inflamatórios de linfonodos, já que fornecem informações no nível celular.

Palavras-chave: Ultrassonografia. Tomografia. Citologia. Linfonodo. Metástase. Cão.

ABSTRACT

ERCOLIN, A. C. M. ***Computed tomographic and B-mode ultrasonographic characteristics of normal, reactive, and neoplastic lymph nodes in dogs.*** 2022. 67 f. Thesis (Doctorate) - Faculdade de Zootecnia e Engenharia de Alimentos, Universidade de São Paulo, Pirassununga, 2022.

A wide range of scientific works described ultrasound and tomographic criteria that contribute to the differentiation between normal and abnormal lymph nodes, both in medicine and in veterinary medicine. However, these studies describe reactive and metastatic lymph nodes in the same group and many have no correlation with gold standard diagnostic methods. The present study investigated if inflammatory and neoplastic processes of canine lymph nodes produce alterations in anatomy and morphology suitable for ultrasonographic and tomographic detection. And, if those alterations found in the imaging exams are exclusive of each process, allowing the differentiation between reactive and neoplastic/metastatic lymph nodes. The first step described a retrospective study on the diagnostic performance of ultrasound for classifying normal lymph nodes as well as benign and malignant lymphadenopathy. 79 cranial cervical lymph nodes and 95 medial iliac and superficial inguinal lymph nodes were evaluated. The accuracy of ultrasonography to detect the status of the lymph nodes varied with the type of lymph node. More than 60% of lymph nodes with distal acoustic enhancement or cystic-like formations were associated with malignancy. In the second part, a systematic review analyzed qualitative evidences to test the hypothesis that computed tomography can differentiate normal lymph nodes from those affected by an inflammatory or metastatic process. Heterogeneous post-contrast enhancement pattern and irregular or indistinct margins may be associated with malignant etiologies. The perinodal fat tissue represents a natural contrasting surface and improves the detection of the lymph node. In general, both modalities benefit from the investigation based on the combination of parameters, such as margin and perinodal fat for tomography and size and echotexture for ultrasound. However, cytology and histopathology are the gold standard methods to diagnose inflammatory and neoplastic lymph nodes, for the provide information at the cellular level.

Keywords: Ultrasound. Computed Tomography. Cytology. Lymph node. Metastasis. Dog.

SUMMARY

1 INTRODUCTION **15**

2 LITERATURE REVIEW **16**

REFERENCES **22**

3 DIAGNOSTIC PERFORMANCE AND CYTOLOGICAL CORRELATION OF B-MODE ULTRASONOGRAPHY IN DIFFERENTIATING CANINE NORMAL, REACTIVE, AND NEOPLASTIC CRANIAL CERVICAL, INGUINAL AND ILIAC LYMPH NODES **24**

ABSTRACT 24

3.1 INTRODUCTION 25

3.2 MATERIAL AND METHODS 26

3.3 RESULTS 29

3.4 DISCUSSION 38

3.5 CONCLUSION 43

REFERENCES 43

4 COMPUTED TOMOGRAPHIC CHARACTERISTICS OF NORMAL, REACTIVE, AND NEOPLASTIC LYMPH NODES IN DOGS: A SYSTEMATIC REVIEW **46**

ABSTRACT 46

4.1 INTRODUCTION 46

4.2 MATERIAL AND METHODS 47

4.3 RESULTS 52

4.4 DISCUSSION 56

4.5 CONCLUSION 61

REFERENCES 62

5 CONCLUSION **64**

APPENDIX 1 **65**

APPENDIX 2 **67**

1 INTRODUCTION

Ultrasonography and tomography are valuable tools to investigate and classify lymph nodes. These imaging modalities have been extensively used to investigate benign and malignant etiologies and are particularly important for tumoral staging and prognosis. Literature offers a wide range of publications describing normal and abnormal lymph nodes but there is some controversy when trying to describe tomographic or ultrasonographic aspects of benign and malignant lymphadenopathies (RUPPEL; POLLARD; WILLCOX, 2019; STAHLE et al., 2019; SILVA et al., 2018). Besides that, most of the studies lack gold standard correlation.

For that reason, our first hypothesis was that B-mode ultrasonography can differentiate normal, reactive and neoplastic lymph nodes in dogs. Thus, the first part of this study aimed to characterize mandibular, medial retropharyngeal, superficial inguinal and medial iliac lymph nodes in dogs, and to assess the diagnostic performance of ultrasonography for the diagnosis of normal, reactive, and neoplastic canine lymph nodes. This first part consisted of a retrospective study with data collected from the University of Florida Veterinary Hospitals. Our object of study consisted of the mandibular and medial retropharyngeal lymph nodes - involved in the drainage of the head and neck in dogs, and the superficial inguinal and medial iliac lymph nodes which participate in the drainage system of the inguinal, lumbosacral and pelvic regions.

This resulted in the first research paper entitled "Diagnostic performance and cytological correlation of B-mode ultrasonography in differentiating canine normal, reactive and neoplastic cranial cervical, inguinal and iliac lymph nodes", presented in the third section of this thesis.

The second part of the study consisted of a systematic review about tomography of canine lymph nodes and involved the tomographic characterization of normal lymph nodes and lymphadenopathies in dogs. Our hypothesis was that tomography can differentiate normal, reactive and neoplastic lymph nodes. This study entitled "Computed tomographic characteristics of normal, reactive, and neoplastic lymph nodes in dogs: a systematic review" is presented in the fourth section of this thesis.

Ultrasonographic exams of mandibular, medial retropharyngeal, superficial

inguinal and medial iliac lymph nodes of clinically healthy dogs were performed and constituted the control group of the study with ultrasonography. This prospective research was conducted at the veterinary hospital UDCH - FZEA - USP in Pirassununga/SP and is presented in the appendix 1.

Additionally, the appendix 2 presents the sinopse of a book chapter about ultrasonography of lymph nodes in dogs, elaborated as a collaboration for the book entitled "Atlas of Ultrasonography in Dogs and Cats", authored by Luciane M. Kanayama, which is being edited.

2 LITERATURE REVIEW

The lymph node is divided in the cortex, which contains lymphoid follicles that produce the lymphocytes, and medulla, consisting of anastomosing cords of macrophages and lymphocytes (FRY; MCGAVIN, 2007). An internal framework is composed by *septae* and *trabeculae* that originate from the fibrous capsule which encloses the lymph nodes and extend into the inner portion of this organ (KONIG; LIEBICH, 2009). Multiple afferent lymphatic vessels pierce the capsule and communicate to the subcapsular sinus. Efferent lymphatic vessels exit the organ at the hilum, together with afferent and efferent blood vessels (FRY; MCGAVIN, 2007).

The lymph nodes are a barrier to the spread of infection and tumors (KONIG; LIEBICH, 2009), participating in the production of immune cells (hematopoietic - lymphopoietic system) and filtration of particulate material such as microorganisms and tumor cells (monocyte-macrophage system) (FRY; MCGAVIN, 2007).

Anatomy of the lymphatic system of the head and neck

Mandibular, parotid and retropharyngeal are the three lymphocenters in the canine head and neck (KONIG; LIEBICH, 2009). Lymph nodes at the parotid and mandibular lymphocenters almost always drain to the medial retropharyngeal lymph nodes. From there, the lymph courses through the tracheal trunk, reaching the thorax (BELZ; HEATH, 1995; KONIG; LIEBICH, 2009) (Figure 1).

The medial retropharyngeal lymph node is located obliquely, dorsomedially and caudally to the mandibular salivary gland and is isoechoic when compared to the gland (NYMAN et al., 2005). These lymph nodes are located lateral to the common carotid artery in the transverse plane (PENNINCK; D'ANJOU, 2015) and caudomedial to the linguofacial bifurcation (WAINBERG; OBLAK; GIUFFRIDA, 2018), draining the pharynx, larynx, cranial part of the trachea and esophagus (KONIG; LIEBICH, 2009).

A study with computed tomography (CT) described the medial retropharyngeal lymph node as the largest lymph node of the head and neck (KNEISSL; PROBST, 2007).

The mandibular salivary gland was described by a CT study as the most useful landmark to identify the medial retropharyngeal lymph node, which is located medially to the caudal aspect of the gland, in a fatty triangle space (KNEISSL; PROBST, 2007).

The mandibular lymph nodes are located between the hemimandibles, draining the oral cavity, tongue, teeth, salivary glands, intermandibular space, and masticatory muscles (KONIG; LIEBICH, 2009). Some authors pointed the facial vein as a landmark to the mandibular lymph node in dogs (KNEISSL; PROBST, 2007).

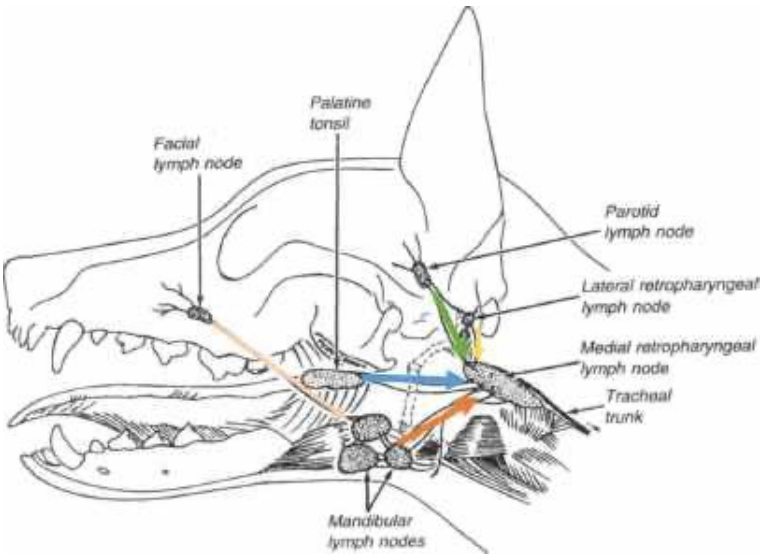

Figure 1. Scheme of the anatomy of the canine head and neck, showing the lymphatic pathway. Adapted from Belz and Heath (1995).

Anatomy of medial iliac and superficial inguinal lymph nodes

Medial iliac lymph nodes are part of the iliosacral lymphocenter, along with the internal iliac (also known as hypogastric) and sacral lymph nodes.

They can be assessed by the flank, between the Psoas major muscle, caudal aorta and caudal vena cava; ventrally to the vertebral body of L5 and L6. The anatomical landmark frequently used is the region where the caudal aorta originates the external iliacs and circumflex arteries, as they are located between the deep circumflex artery and the external iliac arteries (D'ANJOU; CARMEL, 2015).

Afferent lymphatic vessels are originated from the abdominal wall, pelvis, tail root, abdominal, pelvic and lumbar muscles, musculature and bones from the pelvic limbs, large intestines, male and female reproductive systems, urinary bladder, urethra, aorta, superficial inguinal, left colic, sacral and internal iliac lymph nodes. Efferent lymphatic vessels from medial iliac lymph nodes constitute the lumbar lymphatic trunk (BEZUIDENHOUT, 2013).

Superficial inguinal lymph nodes belong to the inguinofemoral lymphocenter. They are located dorsally and laterally to the glans of the penis or deeply to the inguinal mammary glands of females (BEZUIDENHOUT, 2013).

Their afferent lymphatic vessels come from the ventral abdominal wall, abdominal and inguinal mammary glands, penis, prepuce and scrotum, pelvis, tail and pelvic limbs, draining to the medial iliac lymph nodes (BEZUIDENHOUT, 2013).

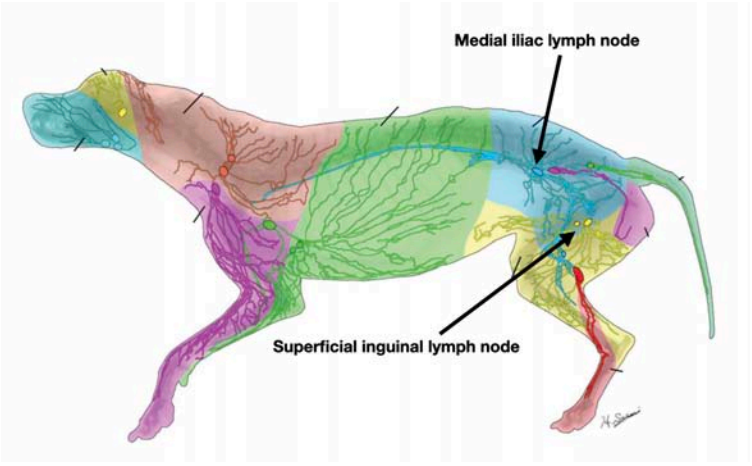

Figure 2. Scheme of the anatomy of the medial iliac and superficial inguinal lymph nodes. Different colors represent different lymphatic territories, according to Suami et al. (2013). Adapted from Suami et al. (2013).

Literature contains a wide collection of studies with descriptions of tomographic and ultrasonographic characteristics to differentiate normal and abnormal lymph nodes. Ultrasonographic criteria most likely related to normal mandibular, medial retropharyngeal, medial iliac, and superficial inguinal lymph nodes in dogs were summarized in the Box 1. Characteristics frequently associated with abnormal canine lymph nodes, regardless of the etiology (benign or malignant), were summarized in Box 2. Tomographic characteristics associated with malignant lymph nodes were summarized in Box 3.

Box 1. Ultrasonographic characteristics of normal canine lymph nodes				
	Mandibular	**Medial retropharyngeal**	**Medial Iliac**	**Superficial Inguinal**
SHAPE	Ovoid (NYMAN et al., 2005)	Fusiform or ovoid (RUPPELL; POLLARD; WILLCOX, 2019)	Fusiform (GANESAN et al., 2016; MAYER; LAWSON; SILVER, 2010; LLABRES-DIAZ, 2004)	Fusiform (MAYER; LAWSON; SILVER, 2010)
HILUM DEFINITION	No difference between malignant and benign lymph nodes (NYMAN et al., 2005; DE SWARTE et al., 2011)			
ECHOGENICITY	Isoechoic to the adjacent tissue (NYMAN et al., 2005) Hypoechoic halo (PENNINCK; D'ANJOU, 2015)	Isoechoic to the adjacent tissue/ salivary gland (RUPPELL; POLLARD; WILLCOX, 2019)	Isoechoic to the adjacent tissue (NYMAN et al., 2006; DE SWARTE et al., 2011) Hypo or isoechoic (MAYER 2010; DE SWARTE et al., 2011)	Hypo or isoechoic (MAYER; LAWSON; SILVER, 2010)
ECHOTEXTURE	Homogeneous or heterogeneous	Homogeneous or heterogeneous	Homogeneous (GANESAN et al., 2016; (MAYER; LAWSON; SILVER, 2010; LLABRES-DIAZ, 2004) Homogeneous or heterogeneous (KINNS; MAI, 2007)	Homogeneous (MAYER; LAWSON; SILVER, 2010) Homogeneous or heterogeneous (KINNS; MAI, 2007)
MARGIM	Regular and defined (NYMAN et al., 2005)	Regular and defined (NYMAN et al., 2005)	Regular and defined (NYMAN et al., 2005; MAYER; LAWSON; SILVER, 2010; DE SWARTE et al., 2011) Hyperechoic capsule (GANESAN et al., 2016)	Regular and defined (NYMAN et al., 2005; MAYER; LAWSON; SILVER, 2010)
PERINODAL FAT	Isoechoic	Isoechoic	Isoechoic (DE SWARTE et al., 2011)	Isoechoic

SIZE	10mmx20mm (CHAURASIA, 2018)	Up to 2,5cm length, 1 cm diameter in transverse view (BURNS, SCRIVANI; THOMPSON, 2008) ratio <0,5	1,58 to 1,69cm length and 0,46 to 0,49cm height (GANESAN et al., 2016) 2,22 to 2,13cm length and 0,46 to 0,48cm height Ratio <0,5 (MAYER; LAWSON; SILVER, 2010)	1,77 to 1,79cm length and 0,31cm height Ratio <0,5 (MAYER; LAWSON; SILVER, 2010) Average 1,5cm NYMAN et al., 2005

Box 2. Ultrasonographic characteristics of abnormal canine lymph nodes with neoplastic or non-neoplastic etiologies	
SHAPE	Rounded, ratio <0,5 (NYMAN et al., 2004; LLABARES-DIAZ, 2004; BELOTTA et al., 2019)
HILUM DEFINITION	Present or absent (NYMAN et al., 2005; DE SWARTE et al., 2011)
ECHOGENICITY	Hypoechoic to the surrounding tissue (NYMAN et al., 2005) Heterogeneous echogenicity (with cystic-like areas - neo and non-neoplastic diseases)
ECHOTEXTURE	Homogeneous or heterogeneous (DE SWARTE et al., 2011; KINNS; MAI, 2007) or heterogeneous(LLABARES-DIAZ, 2004)
MARGIN	Irregular and ill-defined (NYMAN et al., 2005)
PERINODAL FAT	Distal acoustic enhancement (NYMAN et al., 2005) and/ or Hyperechoic perinodal fat (DAVE; ZEKAS; AULD, 2017)
SIZE	Larger short and long axis dimensions (BELOTTA et al., 2019; LLABARES-DIAZ, 2004; DAVE; ZEKAS; AULD, 2017). Superficial lymph nodes with 2cm reactive; 2,5cm with metastasis and 3cm with lymphoma (NYMAN et al., 2005)

Box 3. Tomographic parameters used to characterize lymph nodes
Density (HU differences) (BONAPARTE et al., 2016; HOSTETTLER et al, 2015; STEHLIK et al, 2020; SMITH; SUTTON; MAJOR, 2019)
Compression or invasion of surrounding structures (BONAPARTE et al., 2016)
Localization (BONAPARTE et al., 2016)
Contrast enhancement (BONAPARTE et al., 2016; NEMANIC et al., 2015; STOKOWSKI et al, 2016; HOSTETTLER et al, 2015; STEHLIK et al, 2020)
Size (BONAPARTE et al., 2016; NEMANIC et al., 2015; STOKOWSKI et al, 2016; HOSTETTLER et al, 2015; STEHLIK et al, 2020; SMITH; SUTTON; MAJOR, 2019)
Shape (NEMANIC et al., 2015; STOKOWSKI et al, 2016)
Margins (STEHLIK et al, 2020; NEMANIC et al., 2015)
Presence of hilum (NEMANIC et al., 2015)
Perinodal fat (NEMANIC et al., 2015)
Attenuation (NEMANIC et al., 2015; STOKOWSKI et al, 2016; SMITH; SUTTON; MAJOR, 2019)
Heterogeneity (NEMANIC et al., 2015)
Symmetry (NEMANIC et al., 2015)

Computed tomography was compared to ultrasonography. Advantages and disadvantages of each modality are described in Box 4. Suitable anatomical alterations may not be detected by those imaging modalities in such a way that novel advanced imaging exams or biopsy are required (JONES et al., 2017; LE BLANC; DANIEL; 2007). Some normal appearing lymph nodes may contain micro metastasis. For that reason, some authors recommended aspiration of the ipsilateral and sometimes contralateral regional lymph node to the primary tumor (MAGESTRO; GIEGER, 2016).

Box 4. Comparison between computed tomography and ultrasonography for the detection of lymph nodes: advantages and disadvantages of each modality
CT and MRI are superior to ultrasound in the ability to identify iliosacral lymph nodes (MAJESKI et al, 2017)
CT can detect the origin of masses (STOKOWSKI et al, 2016) or structures missed in US (BONAPARTE et al, 2016)
CT is more accurate to identify affected iliosacral lymph nodes in dogs with apocrine gland adenocarcinoma of the anal sac (where US failed to) (PALLADINO et al, 2016)
Contrast CT identified more normal lymph nodes, whereas the US detected more abnormal lymph nodes (POLLARD; FULLER; STEFFER, 2015)
CT detected in metastasis of insulinoma (where US failed to), but also found false-positives (ROBBEN et al, 2005)
CT and US were ineffective to identify the primary site of insulinoma, requiring intraoperative inspection and palpation of pancreas (ROBBEN et al, 2005)
CT detected more lesions than US in dogs weighing more than 25Kg (FIELDS et al, 2012)
The US can be time-consuming, operator-dependent and influenced by patient factors, such as size and intraperitoneal fat. CT provides a more consistent interpretation of exams (FIELDS et al, 2012) and has better contrast and spatial resolution, which enhancing the detection of soft tissue structures
The US is subjective and has interference from gas artifacts. For that reason this modality is not the adequate for staging and monitoring of most abdominal tumors in humans (FIELDS et al, 2012)
Variation in US measurements intra- and inter-observers can affect treatment and progression of the disease (FIELDS et al, 2012)
CT needs anesthesia to prevent motion artifacts. However new multi-slice CT machines and increased pitches can decrease scan time to a point that enable the use of sedation (FIELDS et al, 2012; BONAPARTE et al, 2016)
US of unsedated animals (the reality in most clinical situations) tend to take longer and has reduced ability of lesion detection (FIELDS et al, 2012)
CT can detect extra-abdominal lesions (FIELDS et al, 2012)
The frequency of abdominal lymph center identification in CT was higher than that observed in US in cats (PERLINI; BUGBEE; SECREST, 2018) and also in dogs (POLLARD; FULLER; STEFFEY, 2015; PALLADINO et al., 2016) because gas and ingesta can cause artifact on US
US=ultrasound; CT=computed tomography; MRI=magnetic resonance imaging

REFERENCES

BELOTTA, A. F.; SUKUT, S.; LOWE, C.*et al*. Computed tomography features of presumed normal mandibular and medial retropharyngeal lymph nodes in dogs. **Canadian Journal of Veterinary Research**, v. 86, p. 27-34, 2022.

BELZ, G. T.; HEATH, T. J. Lymph pathways of the medial retropharyngeal lymph node in dogs. **Journal of Anatomy**, v. 186, p. 517-526, 1995.

BEZUIDENHOUT, A. J. The Lymphatic System. In: Evans HE, Lahunta A, editors. Miller's Anatomy of the dog. 4th ed. St. Louis, MO: Elsevier Saunders; 2013. p. 537-57.

BONAPARTE A.; DHALIWAL, R. S.; HEO, J. *et al*. Whole Body Computed Tomography for Tumor Staging in Dogs: Review of 16 Cases. **Journal of Veterinary Science and Technology,**, v. 7, 2016.

BURNS, G.O.; SCRIVANI, P. V.; THOMPSON, M. S. *et al.* Relation between age, body weight, and medial retropharyngeal lymph node size in apparently healthy dogs. **Veterinary Radiology and Ultrasound**, v. 49, n. 3, p. 277–281, 2008.

CHAURASIA, S.; MENAKA, R.; RAO, T. K. S. *et al*. Clinical Importance of Lymphatic Territories with Special Reference to Mammary Glands and Uterus in Canine: A Review. **Theriogenology Insight**, v. 8, n, 2, p. 79-86, 2018.

D'ANJOU, M. A.; CARMEL, E. N. Abdominal cavity, lymph nodes and great vessels In: Penninck D, d'Anjou MA, editors. Atlas of small animal ultrasonography. 2nd ed. Iowa: Wiley-Blackwell; 2015. p. 455-474.

DAVE, A. C.; ZEKAS, L. J.; AULD, D. M. Correlation of cytologic and histopathologic findings with perinodal echogenicity of abdominal lymph nodes in dogs and cats. **Veterinary Radiology and Ultrasound**, v. 58, p. 463–470, 2017.

DE SWARTE, M.; ALEXANDER, K.; RANNOU, B. *et al.* Comparison of sonographic features of benign and neoplastic deep lymph nodes in dogs. **Veterinary Radiology and Ultrasound,** v. 52, p. 451-456, 2011.

FIELDS, E. L.; ROBERTSON, I. D.; OSBORNE, J. A. *et al*. Comparison of abdominal computed tomography and abdominal ultrasound in sedated dogs. **Veterinary Radiology and Ultrasound,** v. 53, n. 5, p. 513–517, 2012.

FRY, M. M.; McGAVIN, M. D. Bone marrow, blood cells, and lymphatic system. In: McGavin MD, Zachary JF, editors. Pathologic basis of veterinary disease. 4 ed. St. Louis, Mo: Mosby Elsevier; 2007. p. 774-5.

GANESAN, S.; MOHINDROO, J.; VERMA, P. *et al*. Ultrasonographic features of medial iliac and jejunal lymph nodes in apparently healthy dogs. **Turkish Journal of Veterinary and Animal Sciences**, v. 40, p. 225-228, 2016/

HOSTETTLER, F. C.; WIENER, D. J.; WELLE, M. M. *et al*. Post mortem computed tomography and core needle biopsy in comparison to autopsy in eleven Bernese mountain dogs with histiocytic sarcoma. **BMC Veterinary Research,** v. 11, p. 229, 2015.

JONES, I. D.; DANIELS, A. D.; LARA-GARCIA, A. *et al*. Computed tomographic findings in 12 cases of canine multi-centric lymphoma with splenic and hepatic involvement. **Journal of Small Animal Practice,** 2017.

KINNS, J.; MAI, W. Association between malignancy and sonographic heterogeneity in canine and feline abdominal lymph nodes. **Veterinary Radiology and Ultrasound**, v. 48, p. 565-569, 2007.

KNEISSL, S.; PROBST, A. Comparison of computed tomographic images of normal cranial and upper cervical lymph nodes with corresponding E12 plastinated- embedded sections on the dog. **The Veterinary Journal**, v. 174, p. 435-438, 2007.

KONIG, H. E.; LIEBICH, H. G. Immune system and lymphatic organs. In: Konig HE, Liebich HG, editors. Veterinary anatomy of domestic animals. 4 ed. Sttutgart, Germany: Schattauer; 2009. p. 452-4.

LEBLANC, A. K.; DANIEL, G. B. Advanced Imaging for Veterinary Cancer Patients. **Veterinary Clinics of North America: Small Animal Practice,** v. 37, p. 1059–1077, 2007.

LLABRES-DIAZ, F. J. Ultrasonography of the medial iliac lymph nodes in the dog. **Veterinary Radiology and Ultrasound,** v. 45, p.156–165, 2004.

MAGESTRO, L. M.; GIEGER, T. L. Detection of synchronous primary tumours and previously undetected metastases in 736 dogs with neoplasia undergoing CT scans for diagnostic, staging and/ or radiation treatment planning purposes. **Veterinary and Comparative Oncology,** 2016.

MAJESKI, S. A.; STEFFEY, M. A.; FULLER, M. *et al*. Indirect computed tomography lymphography for iliosacral lymphatic mapping in a cohort of dogs with anal sac gland adenocarcinoma: Technique description. **Veterinary Radiology and Ultrasound,** v. 58, n. 3, p. 295–303, 2017.

MAYER, M. N.; LAWSON, J. A.; SILVER, T. I. Sonographic characteristics of presumptively normal canine medial iliac and superficial inguinal lymph nodes in the dog. **Veterinary Radiology and Ultrasound,** v. 51, p. 638–641, 2010.

NEMANIC, S.; HOLLARS, K.; NELSON, N. C. *et al*. Combination of computed tomographic imaging characteristics of medial retropharyngeal lymph nodes and nasal passages aids discrimination between rhinitis and neoplasia in cats. **Veterinary Radiology and Ultrasound,** v. 56, n. 6, p. 617–627, 2015.

NYMAN, H. T.; KRISTENSEN, A. T.; FLAGSTAD, A. *et al*. A review of the sonographic assessment of tumor metastases in liver and superficial lymph nodes. **Veterinary Radiology and Ultrasound**, v. 45, p. 438-448, 2004.

NYMAN, H. T.; KRISTENSEN, A. T.; SKOVGAARD, I. M. *et al*. Characterization of normal and abnormal canine superficial lymph nodes using gray-scale b-mode, color flow mapping, power, and spectral doppler ultra- sonography: a multivariate study. **Veterinary Radiology and Ultrasound,** v. 46, p. 404–410, 2005.

NYMAN, H. T. A.; LEE, M. H.; MCEVOY, F. *et al*. Comparison of B-mode and Doppler ultrasonographic find- ings with histologic features of benign and malignant superficial lymph nodes in dogs. **American Journal of Veterinary Research**, v. 67, p. 978-984, 2006.

PALLADINO, S.; KEYERLEBER, M. A.; KING, R. G. *et al*. Utility of Computed Tomography versus Abdominal Ultrasound Examination to Identify Iliosacral lymphadenomegaly in Dogs with Apocrine Gland Adenocarcinoma of the Anal Sac. **Journal of Veterinary Internal Medicine,** v. 30, p. 1858–1863, 2016.

PENNINCK; D.; D'ANJOU, M. A. **Atlas of Small Animal Ultrasonography**. 2ed. Iowa, USA: Wiley-Blackwell, 2015.

POLLARD, R. E.; FULLER, M. C.; STEFFEY, M. A. Ultrasound and computed tomography of the iliosacral lymphatic centre in dogs with anal sac gland carcinoma. **Veterinary and Comparative Oncology,** v. 15, n. 2, p. 299-306, 2017.

PERLINI, M.; BUGBEE, A.; SECREST, S. Computed tomographic appearance of abdominal lymph nodes in healthy cats. **Journal of Veterinary Internal Medicine**, v. 32, p. 1070–1076, 2018.

ROBBEN, J. H.; POLLAK, Y. W. E. A.; KIRPENSTEIJN, J. *et al*. Comparison of ultrasonography, computed tomography, and single-photon emission computed tomography for the detection and localization of canine insulinoma. **Journal of Veterinary Internal Medicine**, v. 19, p. 15-22, 2005.

RUPPEL, M. J.; POLLARD, R. E.; WILLCOX, J. L. Ultrasonographic characterization of cervical lymph nodes in healthy dogs. **Veterinary Radiology and Ultrasound,** v. 60, p. 560–566, 2019.

SILVA, P.; USCATEGUI, R. A. R.; MARONEZI, M. C. *et al*. Ultrasonography for lymph nodes metastasis identification in bitches with mammary neoplasms. **Scientific Reports**, v. 8, p. 17708, 2018.

SMITH, A. J.; SUTTON, D. R.; MAJOR, A. C. CT appearance of presumptively normal intrathoracic lymph nodes in cats. **Journal of Feline Medicine and Surgery,** p. 1–7, 2019.

STAHLE, J. A.; LARSON, M. M.; ROSSMEISL, J. H. *et al*. Diffusion-weighted magnetic resonance imaging is a feasible method for characterizing regional lymph nodes in canine patients with head and neck disease. **Veterinary Radiology and Ultrasound,** v. 60, p. 176–183, 2019.

STEHLIK, L.; VITULOVA, H.; SIMEONI, F. *et al*. Computed tomography measurements of preseumptively normal canine sternal lymph nodes. **BMC Veterinary Research**, v. 16, p. 269, 2020.

STOKOWSKI, S.; RUTH, J.; LANZ, O. *et al*. Computed Tomographic Features in a Case of Bilateral Neoplastic Cryptorchidism with Suspected Torsion in a Dog. **Frontiers in Veterinary Science,** v. 3, p. 33, 2016.

SUAMI, H.; YAMASHITA, S.; SOTO-MIRANDA, M. A.; CHANG, D. W. Lymphatic territories (lymphosomes) in a canine: An animal model for investigation of postoperative lymphatic alterations. **PLoS ONE**, v. 8, p. e69222, 2013.

WAINBERG, S. H.; OBLAK, M. L.; GIUFFRIDA, M. A. Ventral cervical versus bilateral lateral approach for the extirpation of mandibular and medial retropharyngeal lymph nodes in dogs. **Veterinary Surgery, v.** 47, p. 629-33, 2018.

3 DIAGNOSTIC PERFORMANCE AND CYTOLOGICAL CORRELATION OF B-MODE ULTRASONOGRAPHY IN DIFFERENTIATING CANINE NORMAL, REACTIVE, AND NEOPLASTIC CRANIAL CERVICAL, INGUINAL AND ILIAC LYMPH NODES

ABSTRACT

Ultrasonographic criteria attempting to distinguish normal and abnormal lymph nodes have been developed in human and veterinary medicine. However, those studies frequently describe reactive and neoplastic lymph nodes in the same group, and most of them lack a gold standard correlation. This retrospective descriptive study aimed to investigate the diagnostic performance of the B-mode ultrasonography to differentiate canine cranial cervical, superficial inguinal, and medial iliac lymph nodes in normal, reactive, and neoplastic. Ultrasonographic images from 79 mandibular and medial retropharyngeal and 95 inguinal and medial iliac lymph nodes were evaluated by three observers and classified as normal, reactive, or neoplastic. This classification was compared to cytological diagnosis. Inter-rater agreement as well as the diagnostic performance of B-mode ultrasonography were higher for neoplastic than reactive lymph nodes. More than 60% of the lymph nodes with distal acoustic enhancement or cyst-like formations were associated with malignancy. The absence of a hilum definition may be seen in both reactive and metastatic nodes, thus representing an unreliable parameter for the differentiation of those lymph nodes. Size ($p<0,0001$), margin ($p=0,028$), echotexture ($p<0,0001$), and perinodal fat ($p=0,0008$) were significant for the differentiation of normal, reactive and neoplastic superficial inguinal lymph nodes when compared to cytology. Size ($p<0,0001$)

and echotexture (p<0,0001) for medial iliac, and size (p=0,0001) for mandibular lymph nodes, were significant for the diagnosis of normal, reactive, and neoplastic and when compared to cytology. The accuracy of the ultrasound to differentiate normal, reactive, and neoplastic lymph nodes may be improved by the investigation of combined ultrasonographic features.

Keywords: Dog. Lymph node. Neoplastic. Metastatic. Reactive. Ultrasound.

3.1 INTRODUCTION

Canine head and neck tumors drain to regional lymph nodes, thus frequently metastasizing to the mandibular, medial retropharyngeal, and superficial cervical lymph nodes (RUPPEL; POLLARD; WILLCOX, 2019). Mandibular lymph nodes are superficial nodes associated with the drainage of the oral cavity, tongue and masticatory muscles. They terminate in the medial retropharyngeal lymph nodes which also drain the parotid lymph nodes, larynx, esophagus, and salivary glands, and terminate in the tracheal trunk and thoracic duct (SAAR; GETTY, 1975). The proper identification of metastatic nodes is crucial for the staging of the neoplastic diseases, such as oral malignant melanoma and squamous cell carcinoma (GRIMES et al., 2019), and the determination of the prognosis (SILVA et al., 2018).

Superficial inguinal lymph nodes drain the caudal mammary glands, vulva, scrotum, prepuce, penis, and the pelvic limbs (SAAR; GETTY, 1975). Cutaneous mast cell tumors of the inguinal region (BONAPARTE et al., 2016) or pelvic limb can metastasize to the superficial inguinal lymph nodes. Efferent vessels from the inguinal lymph nodes terminate in the medial iliac lymph nodes and drain the pelvic and perineal region (SAAR; GETTY, 1975). The medial iliac lymph nodes drain the caudodorsal abdominal wall, abdominal and lumbar muscles, pelvis, large intestinal, reproductive and lower urinary tracts and inguinal and iliosacral lymph nodes, and constitute the lumbar lymphatic trunk (SAAR; GETTY, 1975). Literature presented numerous reports of anal sac gland tumors (POLLARD; FULLER; STEFFEY, 2015; PALLADINO et al., 2016) or prostate tumors (SUN et al., 2017) metastasizing to the medial iliac lymph nodes.

The ultrasonographic patterns of presumptive normal cervical lymph nodes (RUPPEL; POLLARD; WILLCOX, 2019), medial iliac and inguinal lymph nodes (MAYER; LAWSON; SILVER, 2010; DE SWARTE et al., 2011) have been described. However, the differentiation of metastatic and healthy lymph nodes using B-mode

qualitative ultrasonography in dogs can be complicated (SILVA et al., 2018; RUPPEL; POLLARD; WILLCOX, 2019; STAHLE et al., 2019), and malignant and benign etiologies may present similar sonographic features, specially at early stages (NYMAN et al., 2006; KINNS; MAI, 2007).

Several studies in human and veterinary medicine developed criteria to differentiate normal versus malignant cervical lymph nodes. Some researchers aimed to distinguish between metastatic and lymphomatous nodes but did not differentiate between normal, neoplastic, and reactive lymph nodes. The various causes of lymphadenopathy, including the presence of micrometastasis, may not be differentiated by ultrasonography (NYMAN et al., 2004).

Cytological and histologic analyses were described as the gold standard to diagnose lymph node metastasis (DE SWARTE et al., 2011; RUPPEL; POLLARD; WILLCOX, 2019; STAHLE et al., 2019). Histopathology was reported to be more sensitive than cytology (WAINBERG; OBLAK; GIUFFRIDA, 2018), but biopsies are not performed as often as fine-needle aspirates, which is considered to be an adequate screening test on clinical settings.

However, the majority of the aforementioned ultrasonographic studies lack cytological and histological correlation. For that reason, the present study hypothesized that B-mode ultrasonography can differentiate between normal, reactive, and neoplastic conditions of the mandibular (MLN), medial retropharyngeal (MRLN), superficial inguinal (SILN), and medial iliac lymph nodes (MILN) in dogs. Cytology will be the gold standard. Therefore, we assessed the diagnostic performance of B-mode ultrasonography, as well as inter-observer agreement for the classification of the lymph nodes.

3.2 MATERIAL AND METHODS

3.2.1 Study sample

The study population consists of ultrasound exams performed in dogs at the University of Florida Small Animal Hospital from 2008 to 2022. Our experimental unit were the mandibular, retropharyngeal, superficial inguinal and medial iliac lymph nodes. Data were retrieved from the archive from the University of Florida Veterinary Hospitals' radiology information system (RIS). The key words used as descriptors to

search for cases within the RIS were: "cervical," "neck," "mandibular," "medial retropharyngeal," 'FNA, "fine needle aspirates" and their combinations; "inguinal," "medial iliac" "superficial inguinal" "iliac," 'FNA, "fine needle aspirates" and their combinations; "SA US" as the modality, and "canine" as the species. Images were obtained from studies performed by board-certified veterinary radiologists, radiology residents or ultrasound technicians closely supervised by a board-certified radiologist.

As inclusion criteria, there were considered (1) lymph nodes with conclusive results from cytologic analysis, classified into normal, reactive (lymphoid hyperplasia and lymphadenitis), or neoplastic (primary neoplasia and metastasis); and (2) cytological exams of lymph nodes previously reported by board-certified clinical pathologists, using samples collected via ultrasound-guided fine needle aspirates using 22- and/or 25G needles and processed using standard cytological techniques; (3) complete medical records; and (4) properly labeled ultrasound images of these lymph nodes, with at least a sagittal image of the lymph nodes to be evaluated. Lymph nodes with non-diagnostic or equivocal results from cytology, incomplete records, such as unlabeled right or left side, or non-diagnostic ultrasound images were excluded.

3.2.2 Classification of the lymph nodes

Three observers (an ACVR board-certified radiologist, an experienced radiologist, and a PhD student) independently classified each of the lymph nodes according to shape, echogenicity, margination, size, echotexture, presence of a well-defined hilum, and aspect of the surrounding fat. The observers were blind to the clinical data and results of cytology. Each of the categories received a number so that the categorical independent variables could be quantified.

The size of the lymph nodes (1. small, 2. normal, or 3. large) was based on the length and height, measured in the longitudinal view; thickness in the sagittal view, and/or the short-to-long axis ratio (S/L ratio) (short and long axis measured in the longitudinal view). The measurements were provided along with the ultrasonographic images in longitudinal and/or transverse view, for the classification of the lymph nodes. The echogenicity of the nodal parenchyma (1. isoechoic, 2. hypoechoic, 3. hyperechoic, or 4. heterogeneous) was compared to the echogenicity

of the mandibular salivary gland (for MLN and MRLN) or to the echogenicity of the adjacent musculature (for MLN, MRLN, SILN, and MILN). The pattern of nodal echotexture or the heterogeneity of the parenchyma (1. homogeneous, or 2. heterogeneous); definition of the hilum (1. well defined, 2. ill defined, or 3. not seen); the echogenicity of the fat tissue surrounding the lymph node (1. normal, or 2. hyperechoic); contour or margination (1. regular, or 2. irregular); and shape (1. fusiform, 2. oval/ elongated, 3. rounded, or 4. other) were also gathered. Based on these evaluations, the lymph nodes were then classified as normal, reactive, or neoplastic.

3.2.3 Statistical analysis

Statistical analyses were conducted using commercial softwares (MedCalc Software Ltd., 2022 and Statistical Analysis System - SAS, 9.4). Cytology was considered the gold standard method for this study.

That was performed a descriptive analysis with frequencies and percentages of each categorical variable from each lymph node, for normal, reactive, and neoplastic lymph nodes. For each parameter, there was considered the classification of the highest accurate evaluator. Proportions of ultrasonographic features were compared among diagnostic categories for each lymph node type considering dichotomous outcomes (i.e. normal vs. reactive, reactive vs. neoplastic, and normal vs. neoplastic). Proportions were estimated with MedCalc using the N-1-Chi-Square test (CAMPBELL, 2007). Significance was set at $P < 0,05$.

The diagnostic performance of ultrasound to correctly classify the lymph nodes was investigated for each observer using the sensitivity (true positive/(true positive + false negative) x 100), specificity (true negative/(true negative + false positive) x 100), positive predictive value (true positive/(true positive + false positive) x 100), negative predictive value (true negative/(true negative + false negative) x 100), and accuracy (agreement between ultrasound and cytology) (ARMBRUST el al., 2012).

The inter-observer agreement was assessed with *Kappa* statistic tests. The independent variables with more than two categories were ordered in an ascending order of intensity, and this order accounted for how apart the observers subjectively

classified each of these variables (i.e.: there was virtually more agreement in case where the answers from observers 1 and 2 were “1. Small” and “2. Normal” than when the answers were “1. Small” and “3. Large”). In that case, there were considered values of weighted *Kappa*. The interpretation of the Kappa coefficient considered the inter-rater agreement as poor (*Kappa* < 0); slight (*Kappa* between 0.00 and 0.20); fair (*Kappa* between 0.21 and 0.40); moderate (*Kappa* between 0.41 and 0.60); substantial (*Kappa* between 0.61 and 0.80); or almost perfect (*Kappa* between 0.81 and 1.00) (LANDIS; KOCH, 1997).

Fisher ’s exact test was used to estimate the association between diagnostic and cytology for each observer. The null hypothesis was that there would be no association between the ultrasonographic diagnostic and cytology. For the independent variables, there was considered the classification from the observer with higher *Kappa* coefficient (accuracy). P-values < 0,05 were considered statistically significant.

The GLIMMIX procedure of SAS was used to investigate the effect of each independent variable in the results from cytology and from ultrasound, for each operator and each lymph node type. The mean value of the scores of each characteristic and the significant difference among normal, reactive, and neoplastic lymph nodes were assessed with MEANS procedure of SAS.

3.3 RESULTS

3.3.1 Demographic data

79 lymph nodes (MLN or MRLN) from 49 dogs met the inclusion criteria and the ultrasonographic images were selected for this study. Median age of the dogs at the time of fine-needle aspiration was 9,5 years (range: 1-17 years). Median body weight was 21,7kg (range 4,2-51,7kg). The study included 14 mixed breed dogs (28,5%); six Labrador retriever (12,24%); German Shepherd, Jack Russell Terrier, Chihuahua, Australian Shepherd, Doberman Pinscher, Cavalier King Charles Spaniel with 2 dogs each (4,08%); American Pit Bull Terrier, English Bulldog, Lhasa Apso, Basenji, Maltese, Border Collie, Catahoula Leopard Hog Dog, Welsh Corgi, Bichon Frise, Spinone Italiano, Shetland Sheepdog, Pug, Miniature Pinscher, French Bulldog, Boston Terrier, Weimaraner, Miniature Schnauzer with 1 dog each (2,04%).

From those, 29 (59,18%) were neutered males, 17 (34,69%) were spayed females, and 3 (6,12%) intact males.

From the 79 cranial cervical lymph nodes evaluated, 25,5% (n=20) were right MRLN, 25,5% (n=20) were left MRLN, 32,9% (n=26) were right MLN, and 16,4% (n=13) were left MLN. The prevalence of neoplastic/metastatic lymph nodes was 21,5% (n=17) and reactive lymph nodes (described as lymphoid hyperplasia) was 58% (n=46). Sixteen lymph nodes (control group) were presumed normal. Lymphoma accounted for 41,2% (n=7) of the neoplastic/metastatic lymph nodes. Other malignant etiologies included oral and nasopharyngeal mast cell tumors, 17,6% (n=3), oral squamous cell carcinoma, 17,6% (n=3), oral melanoma, 11,8% (n=2), thyroid carcinoma, 5,9% (n=1), and osteosarcoma, 5,9% (n=1). In some of the cases, lymphadenopathy was associated with benign etiologies such as functional thyroid adenoma and inflammation/rhinitis or unknown cause. Those lymph nodes were diagnosed as reactive nodes in cytology.

Ultrasonographic images of 95 superficial SILN and medial MILN were selected from 40 dogs. Median age of all dogs at the time of fine-needle aspiration was 8,9 years (range: 1,4-14,3 years). Median body weight was 27,5 kg (range: 5,8-54,5kg). The study included 11 mixed breed dogs (27,5%); five American Pit Bull Terriers (12,5%); four Boxer (10%); 3 English Bulldogs (7,5%); two Golden Retriever, and two Boston Terrier (5% each); Miniature Schnauzer, American Skimo dog, Labrador retriever, Weimaraner, Jack Russell Terrier, Great Dane, Pointer, Doberman Pinscher, Spaniel Welsh Springer, German Shepherd, Rottweiler, American Staffordshire Terrier, and Kerry Blue Terrier with one dog each (2,5%). From those, 21 were neutered males (52,5%), 15 were spayed females (37,5%), three females (7,5%) and one male (2,5%).

From the 95 medial MILN and superficial SILN evaluated, 25,3% (n = 24) were right SILN, 31,6% (n = 30) were left SILN, 21% (n = 20) were right MILN, and 22,1% (n = 21) were left MILN. The prevalence of neoplastic/metastatic lymph nodes was of 35,7% (n = 34) and of 31,6% (n = 30) for reactive lymph nodes (described with lymphoid hyperplasia along with hemorrhage, eosinophilic inflammation or reactive histiocytosis). Presumed normal lymph nodes accounted for 31 (32,6%; control group). Mast cell tumors originating from the pelvic limbs and hips accounted for 19 (55,9%) of the malignant etiologies of neoplastic/metastatic lymph nodes. Other

malignant etiologies included apocrine gland anal sac adenocarcinoma (14,7%, n=5), lymphoma (11,8%, n=4) and mast cell tumor from scrotum/prepuce (5,9%, n=2), and prostate (8,8%, n=3) and urothelial carcinoma (2,9%, n=1). In some of the cases, lymphadenopathy was associated with benign etiologies such as lymphoid hyperplasia, eosinophilic inflammatory reaction, or reactive histiocytosis. Those lymph nodes were diagnosed as reactive nodes in cytology.

3.3.2 Imaging analysis

Frequencies of the classification scores for each ultrasonographic parameter were described in Table 1 and Table 2. Normal MLN tended to have an elongated/ oval shape, whereas most of the normal MRLN, SILN, and MILN were fusiform. Reactive lymph nodes presented a fusiform shape, predominantly, and neoplastic lymph nodes presented a fusiform or elongated shape. Shape was significantly different among normal and reactive MLN and SILN; normal and neoplastic SILN; and reactive and neoplastic MRLN.

Size was significantly different between normal and reactive MLN and MILN, normal and neoplastic MLN, SILN and MILN, and between reactive and neoplastic lymph nodes. Most of the normal lymph nodes were classified as normal size. Conversely, most of the reactive and neoplastic lymph nodes were classified as enlarged, with exception of the reactive SILN which had normal size, predominantly.

There was significant difference in the margination between normal and reactive, and between normal and neoplastic SILN, and among reactive and neoplastic lymph nodes. The majority of normal and reactive MLN, MRLN, SILN, and MILN were classified with regular margins. Most of the neoplastic lymph nodes were assigned irregular margins, with exception of MLN.

Hilum definition was different between normal and reactive MLN, normal MLN, SILN and MILN, as well as reactive and neoplastic SILN presented well defined hilum, predominantly. The hilum was not seen for most of normal MRLN, most reactive MLN, MRLN and MILN; and neoplastic MILN and MRLN. Neoplastic MLN lymph nodes presented an ill-defined or not-seen hilum.

Perinodal fat was different between normal and neoplastic SILN, and between reactive and neoplastic lymph nodes. All normal and reactive lymph nodes, and

neoplastic SILN and MILN presented normal perinodal fat, predominantly. Neoplastic cranial cervical lymph nodes were classified with normal or hyperechoic perinodal fat.

Echogenicity was significantly different between normal and reactive, and among reactive and neoplastic lymph nodes; and contributed to the differentiation between normal and neoplastic MRLN and SILN. Most normal MLN, MRLN, and SILN were hypoechoic to the surrounding tissues. Normal MILN were classified as isoechoic to the surrounding musculature. Reactive lymph nodes were predominantly isoechoic or hypoechoic, regardless of its anatomical location. Neoplastic MRLN presented a heterogeneous echogenicity, whereas neoplastic MLN, SILN, and MILN were predominantly hypoechoic to the adjacent tissues.

Table 1. Number and percentage of normal, reactive and neoplastic mandibular and medial retropharyngeal lymph nodes detected for each ultrasonographic category of classification

		Mandibular lymph node			Medial retropharyngeal lymph node		
		Normal (n=13)	**Reactive (n=23)**	**Neoplastic (n=4)**	**Normal (n=3)**	**Reactive (n=23)**	**Neoplastic (n=13)**
Shape	Fusiform	2 (15%)*	12 (52%)*	2 (50%)	2 (66%)	13 (56%)	4 (30%)
	Elongated/oval	10 (77%)*	9 (39%)*	1 (25%)	1 (33%)	9 (39%)	5 (38%)
	Rounded	1 (8%)	1 (9%)	1 (25%)	0	0	0
	Other	0	0	0	0	1 (4%)*	4 (30%)*
Echogenicity	Isoechoic	2 (15%)	8 (34%)	1 (25%)	0	11 (48%)	4 (30%)
	Hypoechoic	10 (77%)	10 (43%)	2 (50%)	2 (66%)	8 (35%)	2 (15%)
	Hyperechoic	1 (8%)	0	0	1 (33%)*	0	0
	Heterogeneous	0	5 (22%)	1 (25%)	0	4 (17%)*	7 (54%)*
Margin	Regular	9 (69%)	19 (83%)	3 (75%)	3 (100%)	17 (74%)	6 (46%)
	Irregular	4 (31%)	4 (17%)	1 (25%)	0	6 (26%)	7 (54%)
Size	Small	0	0	0	0	0	0
	Normal	11 (85%)*	6 (26%)*	1 (25%)*	2 (66%)	9 (39%)	3 (23%)
	Large	2 (15%)*	17 (74%)*	3 (75%)*	1 (33%)	14 (61%)	10 (77%)
Echotexture	Homogeneous	12 (92%)*	17 (74%)	1 (25%)*	3 (100%)	14 (61%)	6 (46%)
	Heterogeneous	1 (8%)*	6 (26%)	3 (75%)*	0	9 (39%)	7 (54%)
Hilum definition	Well defined	10 (77%)*	7 (30%)*	0	0	2 (9%)	1 (7%)
	Ill defined	2 (15%)	6 (26%)	2 (50%)	1 (33%)	8 (35%)	4 (31%)

	Not seen	1 (8%)*	10 (43%)*	2 (50%)	2 (66%)	13 (56%)	8 (61%)
Perinodal fat	Normal	10 (77%)	16 (69%)	2 (50%)	3 (100%)	21 (91%)*	6 (46%)*
	Hyperechoic	3 (23%)	7 (30%)	2 (50%)	0	2 (9%)*	7 (54%)*
	N-1 Chi-square test * Significant difference between groups (P<0,005)						

Table 2. Number and percentage of normal, reactive and neoplastic superficial inguinal and medial iliac lymph nodes detected for each ultrasonographic category of classification

		Superficial inguinal lymph node			Medial iliac lymph node		
		Normal (n=18)	**Reactive (n=17)**	**Neoplastic (n=19)**	**Normal (n=13)**	**Reactive (n=13)**	**Neoplastic (n=15)**
Shape	Fusiform	14 (78%)*	12 (70%)	7 (37%)*	8 (61%)	7 (54%)	7 (47%)
	Elongated/ oval	4 (22%)	5 (29%)	7 (37%)	5 (38%)	5 (38%)	8 (53%)
	Rounded	0	0	1 (5%)	0	1 (8%)	0
	Other	0	0	4 (21%)*	0	0	0
Echogenicity	Isoechoic	7 (39%)*	7 (41%)*	0	7 (54%)	4 (31%)	6 (40%)
	Hypoechoic	10 (55%)	8 (47%)	11 (58%)	3 (23%)	7 (54%)	9 (60%)
	Hyperechoic	1 (5%)	0	1 (5%)	3 (23%)	2 (15%)	0
	Heterogeneous	0	2 (12%)*	7 (37%)*	0	0	0
Margin	Regular	18 (100%)*	10 (59%)*	5 (26%)*	13 (100%)*	12 (92%)*	7 (47%)*
	Irregular	0	7 (41%)*	14 (74%)*	0	1 (8%)*	8 (53%)*
Size	Small	1 (5%)	0	0	0	1 (8%)	0
	Normal	17 (94%)*	12 (70%)	8 (42%)*	11 (85%)*	4 (31%)*	5 (33%)*
	Large	0	5 (29%)*	11 (58%)*	2 (15%)*	8 (61%)*	10 (67%)*
Echotexture	Homogeneous	18 (100%)*	10 (59%)*	10 (53%)*	13 (100%)*	12 (92%)	11 (73%)*
	Heterogeneous	0	7 (41%)*	9 (47%)*	0	1 (8%)	4 (27%)*
Hilum definition	Well defined	10 (55%)	13 (76%)	12 (63%)	7 (54%)	4 (31%)	4 (27%)
	Ill defined	1 (5%)	0	3 (16%)	0	0	0
	Not seen	7 (39%)	4 (23%)	4 (21%)	6 (46%)	9 (69%)	11 (73%)

Perinodal fat	Normal	17 (94%)	15 (88%)	12 (63%)*	11 (85%)	12 (92%)	12 (80%)
	Hyperechoic	1 (5%)*	2 (12%)	7 (37%)*	2 (15%)	1 (8%)	3 (20%)
	N-1 Chi-square test * Significant difference between groups (P<0,005)						

In this study, cases of heterogeneous echogenicity were marked for the presence of distal acoustic enhancement and/or cyst-like structures. Those specific alterations were not contemplated in the list of parameters for the classification of the lymph nodes. However, it is worth mentioning that 64% of the SILN and MILN and 60% of the MLN and MRLN with distal acoustic enhancement or cyst-like structures (Figure 3) were associated with metastatic/neoplastic etiologies.

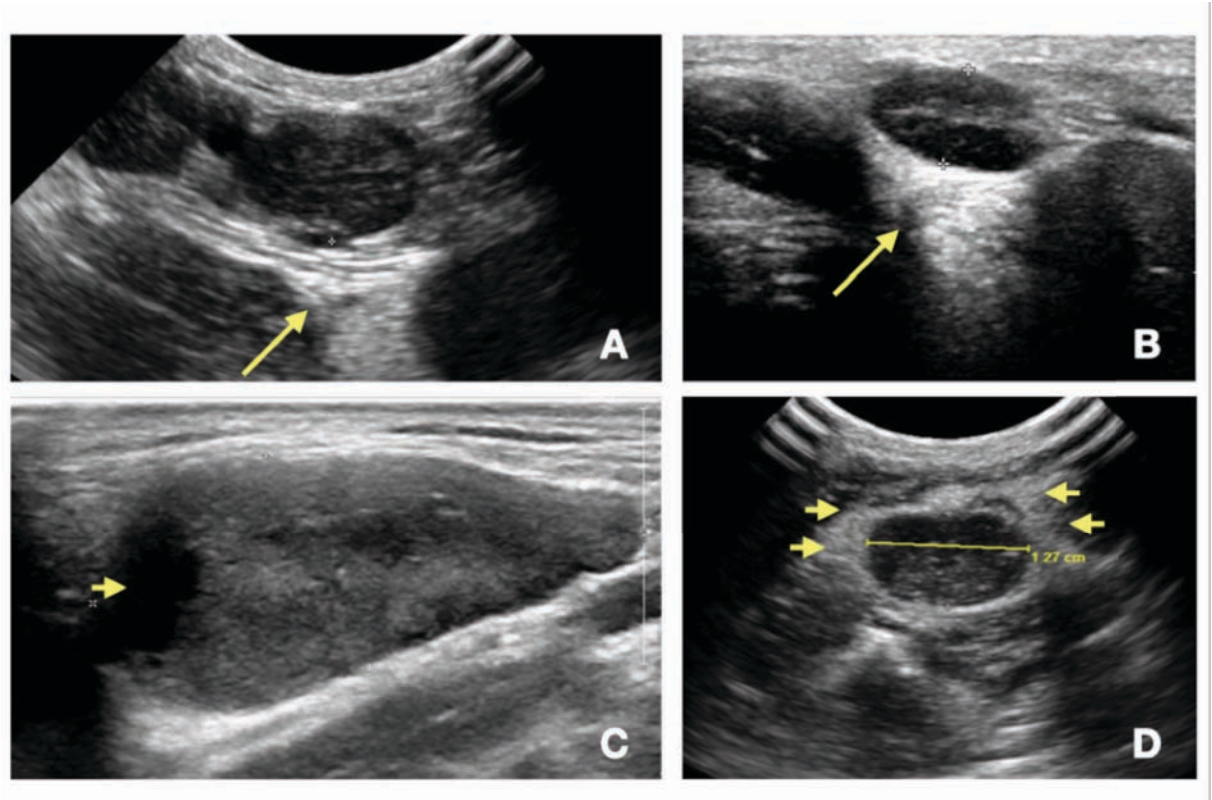

Figure 3: B-mode ultrasonographic images of lymph nodes with morphological features commonly associated with malignant or reactive etiologies. (A) and (B) present distal acoustic enhancement (arrow); (C) present a cyst-like structure (arrow) and (D) shows hyperechoic perinodal fat tissue. University of Florida, Veterinary Hospitals.

The texture was different between normal and reactive SILN; normal and neoplastic MILN and MLN; and reactive and neoplastic lymph nodes. Almost all the normal lymph nodes as well as most of the reactive lymph nodes, and the neoplastic

cranial cervical lymph nodes were classified as homogeneous according to the echotexture of the parenchyma. The parenchyma of neoplastic SILN and MILN were classified as heterogeneous.

There was significant association between B-mode ultrasound and cytology for the diagnosis of normal and neoplastic, but not for reactive lymph nodes. Those results were consistent among observers (Table 3).

Table 3 - P-value for the agreement among each observer and the gold standard method for the classification lymph nodes in normal, reactive, and neoplastic

	Normal	Reactive	Neoplastic
Observer 1	0,00000*	0,09	0,0028*
Observer 2	0,00000038*	0,301	0,00107*
Observer 3	0,00019*	0,359	0,020*
	Fisher exact test *Significance at P<0,005		

B-mode ultrasound was more sensitive to detect normal MILN and MLN (76,92%) than the others. More specific (97,22%) and accurate (89,44%) to detect normal MRLN (Table 4). Ultrasound was more specific (88,24%) to detect reactive MLN when compared to the others. More sensitive (69,57%) for reactive MRLN and more accurate (65,84%) to detect reactive MILN (Table 5). Ultrasound was more sensitive (52,63%) for neoplastic SILN. More specific (94,44%) and accurate (90%) for MLN, when compared to the others (Table 6). Regarding the overall diagnostic performance, ultrasonographic accuracy was higher for detection of normal and neoplastic lymph nodes when compared to reactive lymph nodes for all types of lymph nodes evaluated.

Table 4. Diagnostic performance of the ultrasound to detect normal lymph nodes

	SUPERFICIAL INGUINAL		MEDIAL ILIAC		MANDIBULAR		MEDIAL RETROPHARYNGEAL	
		95% CI		**95% CI**		**95% CI**		**95% CI**
Sensitivity	72.22%	46.52% to 90.31%	76.92%	46.19% to 94.96%	76.92%	46.19% to 94.96%	0.00%	0.00% to 70.76%
Specificity	83.33%	67.19% to 93.63%	71.43%	51.33% to 86.78%	85.19%	66.27% to 95.81%	97.22%	85.47% to 99.93%

Disease prevalence	33.00%		32.00%		32.00%		8.00%	
Positive Predictive Value	68.10%	49.34% to 82.39%	55.89%	39.64% to 70.96%	70.96%	48.53% to 86.36%	0	
Negative Predictive Value	85.90%	74.03% to 92.86%	86.80%	70.35% to 94.80%	88.69%	74.17% to 95.54%	91.79%	91.36% to 92.20%
Accuracy	79.67%	66.51% to 89.40%	73.19%	57.07% to 85.79%	82.54%	67.27% to 92.69%	89.44%	75.40% to 96.98%

Table 5. Diagnostic performance of the ultrasound to detect reactive lymph nodes

	SUPERFICIAL INGUINAL		**MEDIAL ILIAC**		**MANDIBULAR**		**MEDIAL RETROPHARYNGEAL**	
		95% CI		**95% CI**		**95% CI**		**95% CI**
Sensitivity	58.82%	32.92% to 81.56%	61.54%	31.58% to 86.14%	34.78%	16.38% to 57.27%	69.57%	47.08% to 86.79%
Specificity	67.57%	50.21% to 81.99%	67.86%	47.65% to 84.12%	88.24%	63.56% to 98.54%	50.00%	24.65% to 75.35%
Disease prevalence	31.00%		32.00%		57.00%		59.00%	
Positive Predictive Value	44.90%	30.65% to 60.04%	47.39%	31.15% to 64.21%	79.67%	48.72% to 94.17%	66.69%	53.36% to 77.80%
Negative Predictive Value	78.51%	66.48% to 87.06%	78.94%	64.29% to 88.64%	50.51%	41.95% to 59.04%	53.31%	34.16% to 71.53%
Accuracy	64.86%	50.67% to 77.36%	65.84%	49.39% to 79.90%	57.77%	41.15% to 73.19%	61.54%	44.62% to 76.64%

Table 6. Diagnostic performance of the ultrasound to detect neoplastic lymph nodes

	SUPERFICIAL INGUINAL		**MEDIAL ILIAC**		**MANDIBULAR**		**MEDIAL RETROPHARYNGEAL**	
		95% CI		**95% CI**		**95% CI**		**95% CI**
Sensitivity	52.63%	28.86% to 75.55%	26.67%	7.79% to 55.10%	50.00%	6.76% to 93.24%	30.77%	9.09% to 61.43%
Specificity	91.43%	76.94% to 98.20%	92.31%	74.87% to 99.05%	94.44%	81.34% to 99.32%	92.31%	74.87% to 99.05%
Disease prevalence	35.00%		36.00%		10.00%		33.00%	

Positive Predictive Value	76.78%	50.82% to 91.36%	66.10%	28.78% to 90.39%	50.00%	15.90% to 84.10%	66.33%	29.25% to 90.37%
Negative Predictive Value	78.19%	68.82% to 85.34%	69.11%	61.79% to 75.59%	94.44%	86.41% to 97.85%	73.02%	64.95% to 79.82%
Accuracy	77.85%	64.48% to 88.01%	68.68%	52.31% to 82.23%	90.00%	76.34% to 97.21%	72.00%	55.34% to 85.16%

The overall inter-observer agreement for the classification of normal lymph nodes was fair (ranging from 0,213 to 0,376). For the classification of reactive lymph nodes there was a slight agreement between observers (ranging from 0,022 to 0,179). The highest agreement was for the classification of neoplastic lymph nodes (moderate, ranging from 0,33 to 0.55) (Table 7).

Table 7 - Agreement among 3 observers in the classification of ultrasonographic images of 174 lymph nodes in normal, reactive, and neoplastic

	Observers 1 and 2		**Observers 2 and 3**		**Observers 1 and 3**	
Normal	63% (*k*=0,318)	FAIR	67% (*k*=0,376)	FAIR	66% (*k*=0,213)	FAIR
Reactive	53% (*k*=0,022)	SLIGHT	59% (*k*=0,179)	SLIGHT	53% (*k*=0,056)	SLIGHT
Neoplastic	77% (*k*=0,426)	MODERATE	89% (*k*=0,55)	MODERATE	74% (*k*=0,33)	FAIR
Cohen-Kappa statistic test						

The characteristics that significantly contributed to the differentiation in normal, reactive, and neoplastic were presented as mean scores in Table 8. For SILN, size (p<0,0001), margin (p=0,028), echotexture (p<0,0001), and perinodal fat (p=0,0008) were significant for the diagnostic of normal, reactive, and neoplastic and when compared to cytology. For MILN, size (p<0,0001) and echotexture (p<0,0001) were significant for the diagnosis of normal, reactive, and neoplastic and when compared to cytology. For MLN, size (p=0,0001) was the only characteristic significant for both diagnostic and cytology. For MRLN, none of the characteristics was significant to differentiate normal, reactive and neoplastic, according to cytology.

Table 8. Mean score for characteristics that significantly contributed to the differentiation of normal reactive and neoplastic lymph nodes

Lymph node	Characteristic	Normal	Reactive	Neoplastic	P-value
Superficial inguinal	Size	1,97	2,21	2,78	p<0,0001
	Margin	1,09	1,51	1,78	p=0,028
	Echotexture	1,05	1,41	1,82	p<0,0001
	Perinodal fat	1,01	1,25	1,50	p=0,0008
Medial iliac	Size	1,93	2,55	2,84	p<0,0001
	Echotexture	1,00	1,13	1,60	p<0,0001
Mandibular	Size	2,02	2,48	2,92	p=0,0001
Medial retropharyngeal	Echotexture	1,02	1,35	1,83	p=0,0314*
	Perinodal fat	1,00	1,09	1,56	p=0,0136*

Significance at P<0,005 *No significant association with cytology

There was a significant effect of the operator (p=0,024) during evaluation of MILN. Operator effect was not significant for SILN, MLN and MRLN.

3.4 DISCUSSION

Our results showed that normal lymph nodes presented elongated/oval (MLN) or fusiform shape, in accordance with literature (NYMAN et al.,2005; MAYER; LAWSON; SILVER, 2010; SILVER et al., 2012; RUPPEL; POLLARD; WILLCOX, 2019). Reactive lymph nodes were mostly fusiform, compared to previous reports of ovoid shape for normal and reactive superficial lymph nodes (NYMAN et al., 2004; NYMAN et al., 2005). Our results agree with previous statements that reactive lymph nodes are usually oval, with a short-to-long axis ratio < 0.5 (NYMAN et al., 2005; KNEISSL; PROBST, 2006). We found that neoplastic lymph nodes were elongated/ oval or fusiform, predominantly. Conversely, studies described rounded neoplastic and metastatic superficial lymph nodes (NYMAN et al., 2004; LLABRES-DIAZ, 2004;

SILVA et al., 2018; BELOTTA et al., 2019), with a short-to-long axis ratio > 0.5 (STAN et al, 2020).

In our study, observers used the measurements of length, height, diameter, or short-to-long axis ratio to classify each lymph node according to size (small, normal, or large). However, we are not evaluating the effect of specific measurements, which have already been extensively reported in literature (SILVA et al., 2018; BELOTTA et al., 2019). Instead, we considered the final classification in "small", "normal" or “large”.

Neoplastic lymph nodes had larger dimensions when compared to benign lymph nodes in both dogs and cats (DAVE; ZEKAS; AULD, 2017). Conversely, in the present study, most of the reactive and neoplastic lymph nodes were enlarged, corroborating with other authors (KINNS; MAI, 2007; BELOTTA et al., 2019). Therefore, size is not reliable to differentiate reactive and neoplastic lymph nodes. We highlight the importance of associating other sonographic features such as shape and margination, considering that reactive lymph nodes present diffuse alterations and a uniform enlargement (SILVA et al., 2018), whereas neoplastic changes maybe focal or diffuse and this enlargement normally prompts to irregular margins (SILVA et al., 2018; STAN et al., 2020).

In the present study, normal and reactive lymph nodes presented regular margins whereas most of neoplastic (except for MLN) had irregular margins. Some authors mentioned no statistical difference for margination between benign and malignant lymph nodes (NYMAN et al., 2005; BELOTTA et al., 2019). Besides that, regular smooth margins may be associated with benign etiologies and irregular sharp margins tend to relate to malignant lymph nodes (NYMAN et al., 2005). Again, any focal protuberance, irregular contour or distortion of the shape could indicate tumor infiltration. Comparatively, reactive lymph nodes, such as those presenting an inflammatory process, tend to preserve the shape even when enlarged (SILVA et al., 2018).

The detection of an echogenic hilum was challenging for a significant amount of lymph nodes in our study, regardless of the diagnostic. Previous statements support these findings mentioning that the hilum can be missed in cases of inflammatory and neoplastic lymph nodes with a heterogeneous pattern with hypoechoic and hyperechoic zones (RUBALTELLI et al., 1990; NYMAN et al., 2005),

and normal small-sized lymph nodes in humans (YING et al., 2001). The evaluation of the hilum can be affected by size of the dogs or depth of the target lymph node (DE SWARTE, 2011). Our results showed that some normal, reactive, and neoplastic lymph nodes presented a well-defined hilum. In addition, in our retrospective study, we used saved static images to obtain the lymph nodes' measurements and other features. Given that, the absence of visualization of a hilar region in our study may simply indicate that the available images of the lymph nodes may not contain the hilus, not being related to the degree of conspicuity of the hilar region. Furthermore, the detection or absence of a well-defined hyperechoic hilum did not differ from malignant to benign lymph nodes in dogs (NYMAN et al., 2005; NYMAN et al., 2006; BELOTTA et al., 2019).

We found that perinodal fat was normal or iso/hypoechoic to the lymph nodes parenchyma for normal, reactive and most of the neoplastic nodes, except for some cranial cervical (that presented adjacent hyperechoic fat). Normal perinodal fat was previously associated with benign nodes in both dogs and cats. Interestingly, hyperechoic perinodal fat was related to round cell neoplasia in dogs and with reactive lymph nodes in cats (DAVE, ZEKAS; AULD, 2017). Other studies reported non-statistical differences for perinodal fat between malignant and benign nodes, although hyperechoic perinodal fat was more frequently associated with malignant etiologies (BELOTTA et al., 2019).

Normal MLN, MRLN, and SILN were hypoechoic to the surrounding tissues. The echogenicity of normal MILN was isoechoic to the surrounding musculature (MAYER; LAWSON; SILVER, 2010; SILVER et al., 2012). Reactive lymph nodes were isoechoic or hypoechoic to the adjacent tissues. Neoplastic MRLN had a heterogeneous echogenicity while neoplastic mandibular, inguinal and medial iliac were hypoechoic. Reactive superficial lymph nodes were reported as mixed echogenicity while neoplastic lymph nodes were reported as hypoechoic (NYMAN et al., 2006). Echogenicity was reported as an unreliable parameter to differentiate benign and malignant lymph nodes (DE SWARTE et al., 2011; SILVA et al., 2018). This characteristic can be influenced by operator, patient and depth of the target structures, as confounding factors (DE SWARTE et al., 2011).

Some cases of heterogeneous echogenicity were associated with the presence of cyst-like structures (Figure 1). This imaging finding was not initially

contemplated in our classification system, but was found to be usually associated with metastatic/neoplastic etiologies. These results corroborate with studies that associated distal acoustic enhancement with malignancy in dogs (NYMAN et al., 2005), and lymphoma in humans (AHUJA; YING, 2000). We highlight the importance of distinguishing distal acoustic enhancement (fig. 1A-B) and perinodal hyperechoic fat tissue (fig. D), which can be either associated with reactive or metastatic lymph nodes. Some authors pointed out the limitations of still images to evaluate the uniformity of the nodal parenchyma and the possibility of missing some important features such as cystic formations or cavitations (KINNS; MAI, 2007).

The echotexture was homogeneous for normal and reactive lymph nodes and cranial cervical neoplastic lymph nodes. Neoplastic SILN and MILN were usually heterogeneous. Previous studies associated heterogeneity with malignancy in dogs (LLABRES-DIAZ, 2004; KINNS; MAI, 2007). Other authors reported that both reactive and neoplastic lymph nodes presented a mixed texture of the parenchyma (NYMAN et al., 2006). This parameter was found to be unreliable to differentiate lymph nodes (SILVA et al., 2018) because it can be influenced by the type, location, and staging of the primary tumor, or by the use of high frequency probes which increase spatial resolution that favors a more detailed investigation (DE SWARTE et al., 2011). Neoplastic lymph nodes were reported as homogeneous or heterogeneous (DE SWARTE et al., 2011). Heterogeneous lymph nodes were more frequently malignant but despite this fact, no statistical difference was found between parenchymal uniformity of superficial lymph nodes and malignancy (BELOTTA el al., 2019). Furthermore, heterogeneity in benign nodes may be associated with inflammation whereas it can be related to necrosis in malignant lymph nodes (BELOTTA et al., 2019).

Sensitivity was higher for normal lymph nodes. The lowest sensitivity was found for reactive MLN and MRLN, and neoplastic SILN and MILN. Specificity was higher for normal MRLN, and neoplastic MLN, SILN and MILN. Lowest values were found for reactive lymph nodes. In order to stage a disease, it is preferable to have higher sensitivity (HOANG et al., 2013).

Accuracy was higher for normal and neoplastic lymph nodes when compared to reactive lymph nodes. These findings corroborate with the well-established

consensus that reactive lymph nodes share numerous characteristics with normal and neoplastic nodes, thus they still cannot be completely differentiated.

Inter-rater agreement was more expressive for neoplastic lymph nodes (moderate agreement). There was fair agreement between observers to classify reactive lymph nodes. These findings highlight the fact that reactive lymph nodes share characteristics with both normal and neoplastic lymph nodes, leading to misclassification of these lymph nodes.

B-mode ultrasonography was reported to be inaccurate to replace cytology (BELOTTA et al., 2019), which offered 100% sensitivity and 96% specificity for assessment of lymph node metastasis in dogs and cats with solid tumors (LANGENBACH et al., 2001). Besides that, the combination of features may increase the sonographic diagnostic accuracy for the detection of neoplastic lymph nodes. There were significant effects in the differentiation of the lymph nodes when associating margin and perinodal fat for normal SILN lymph nodes; margin and size for reactive SILN; and size alone for neoplastic SILN and normal MLN; margin and echotexture for neoplastic MILN; and perinodal fat for neoplastic MRLN. The aspect of the margin and appearance of the perinodal fat combined were reported as significant (P=0,03) to differentiate benign and malignant lymph nodes (DE SWARTE et al., 2011). Size, vascular flow distribution and the pulsatility index were reported as important in the differentiation of normal, reactive, neoplastic, and metastatic superficial and abdominal lymph nodes (NYMAN et al., 2005). Other authors suggested the combination of B-mode ultrasonography and other modalities such as elastography can improve accuracy to detect nodal malignancy (BELOTTA et al., 2019).

There were some effects related to the observers for the evaluation of MILN. We suggest that its anatomical location, comparatively deeper than the other lymph nodes evaluated (MLN, MRLN, and SILN), may have influenced the variability among observers. Also, instead of still images, a dynamic evaluation would have potentially contributed to the evaluation and classification of this lymph node. The evaluation of static images represented a limitation of this retrospective study considering that dynamic images would provide more detailed investigation of the different parameters, such as margin or hilum definition. Similar considerations were

previously reported for ultrasonographic investigation of iliosacral lymphadenomegaly in dogs with anal sac gland adenocarcinoma (PALLADINO et al., 2016).

Lymph nodes are submitted to sample collection if presenting a clinical reason. This fact could lead to selection bias of the lymph nodes that are submitted to fine needle aspiration, even though some of the presumed affected lymph nodes presented normal results from cytology.

The interactions between age and body weight and the size of the lymph nodes were not investigated in the present study. Considering the wide variation between age and bodyweight of the dogs routinely evaluated, that influence was considered by some authors to be clinically irrelevant (KNEISSL; PROBST, 2006).

3.5 CONCLUSION

The ultrasonographic classification of reactive lymph nodes is still controversial and relies on cytology or results from biopsy to be confirmed. Besides that, the accuracy of the ultrasound to differentiate normal, reactive and neoplastic lymph nodes could be greatly improved by the investigation of combined features and those could be next steps of the study. The presence of distal acoustic enhancement and cyst-like formations may also be a good indicator of malignant etiologies, recommending that further tissue sampling should be pursued.

ACKNOWLEDGMENTS

Authors would like to thank Luciane Kanayama for collaboration with imaging evaluations. This study was supported by the Coordination for the Improvement of Higher Education Personnel, Brazilian Ministry of Education (CAPES PDSE process 88887.368578/2019-00) and Sao Paulo Research Foundation (FAPESP, process 2020/04868-9) fellowships to Anna C. M. Ercolin.

CONFLICT OF INTEREST

Authors declare no conflict of interest.

REFERENCES

AHUJA, A.; YING, M. Grey-scale sonography on the assessment of cervical lymphadenopathy: a review of sonographic appearances and features that may help a beginner. **British Journal of Oral and Maxillofacial Surgery**, v. 38, p. 451-459, 2000.

ARMBRUST, L. J.; BILLER, D. S.; BAMFORD, A. *et al*. Comparison of three-view thoracic radiography and computed tomography for detection of pulmonary nodules in dogs with neoplasia. **Journal of the American Veterinary Medical Association**, v. 240, p. 1088–1094, 2012.

BELOTTA, A. F.; GOMES, M. C.; ROCHA, N. S. *et al*. Sonography and sonoelastography in the detection of malignancy in superficial lymph nodes of dogs. **Journal of Veterinary Internal Medicine**, v. 33, p. 1403–1413, 2019.

BONAPARTE, A.; DHALIWAL, R. S.; HEO, J. *et al*. Whole Body Computed Tomography for Tumor Staging in Dogs: Review of 16 Cases. **Journal of Veterinary Science and Technology**, v. 7, p. 4, 2016.

CAMPBELL, I. Chi-squared and Fisher-Irwin tests of two-by-two tables with small sample recommendations. **Statistics in Medicine,** v. 26, p. 3661-3675, 2007.

DAVE, A. C.; ZEKAS, L. J.; AULD, D. M. Correlation of cytologic and histopathologic findings with perinodal echogenicity of abdominal lymph nodes in dogs and cats. **Veterinary Radiology and Ultrasound**, v. 58, p. 463–470, 2017.

DE SWARTE, M.; ALEXANDER, K.; RANNOU, B. *et al*. Comparison of sonographic features of benign and neoplastic deep lymph nodes in dogs. **Veterinary Radiology and Ultrasound**, v. 52, p. 451-456, 2011.

GRIMES, J. A.; MESTRINHO, L. A.; BERG, J. *et al*. Histologic evaluation of mandibular and medial retropharyngeal lymph nodes during staging of oral malignant melanoma and squamous cell carcinoma in dogs. **Journal of the American Veterinary Medicine Association**, v. 254, n. 8, p. 938-943, 2019.

HOANG, J. K.; VANKA, J.; LUDWIG, B. J. *et al*. Evaluation of cervical lymph nodes in head and neck cancer with CT and MRI: tips, traps, and a systematic approach. **American Journal of Roentgenology**, v. 200, p. W17-W25, 2013.

KNEISSL, S.; PROBST, A. Magnetic Resonance Imaging features of presumed normal head and neck lymph nodes in dogs. **Veterinary Radiology and Ultrasound**, v. 47, p. 538-541, 2006.

KINNS, J.; MAI, W. Association between malignancy and sonographic heterogeneity in canine and feline abdominal lymph nodes. **Veterinary Radiology and Ultrasound**, v. 48, p. 565-569, 2007.

LANDIS, J. R.; KOCH, G. G. Measurement of observer agreement for categorical data. **Biometrics**, v. 33, n. 1, p. 159-174, 1977.

LANGENBACH, A.; MAC MANUS, P. M.; HENDRICK, M. J. *et al*. Sensitivity and specificity of methods of assessing the regional lymph nodes for evidence of metastasis in dogs and cats with solid tumors. **Journal of the American Veterinary Medicine Association**, v. 218, p. 1424-1428, 2001.

LLABRES-DIAZ, F. J. Ultrasonography of the medial iliac lymph nodes in the dog. **Veterinary Radiology and Ultrasound**, v. 45, p.156–165, 2004.

MAYER, M. N.; LAWSON, J. A.; SILVER, T. I. Sonographic characteristics of presumptively normal canine medial iliac and superficial inguinal lymph nodes. **Veterinary Radiology and Ultrasound**, v. 51, p. 638–641, 2010.

NYMAN, H. T.; KRISTENSEN, A. T.; FLAGSTAD, A. *et al*. A review of the sonographic assessment of tumor metastases in liver and superficial lymph nodes. **Veterinary Radiology and Ultrasound**, v. 45, p. 438-448, 2004.

NYMAN, H. T.; KRISTENSEN, A. T.; SKOVGAARD, I. M. *et al*. Characterization of normal and abnormal canine superficial lymph nodes using gray-scale B-mode, color flow mapping, power, and spectral Doppler ultrasonography: a multivariate study. **Veterinary Radiology and Ultrasound**, v. 46, p. 404-410, 2005.

NYMAN, H. T. A.; LEE, M. H.; MCEVOY, F. *et al*. Comparison of B-mode and Doppler ultrasonographic find- ings with histologic features of benign and malignant superficial lymph nodes in dogs. **American Journal of Veterinary Research**, v. 67, p. 978-984, 2006.

PALLADINO, S.; KEYERLEBER, M. A.; KING, R. G. *et al*. Utility of computed tomography versus abdominal ultrasound examination to identify iliosacral lymphadenomegaly in dogs with apocrine gland adenocarcinoma of the anal sac. **Journal of Veterinary Internal Medicine**, v. 30, p. 1858–1863, 2016.

POLLARD, R. E.; FULLER, M. C.; STEFFEY, M. A. Ultrasound and computed tomography of the iliosacral lymphatic centre in dogs with anal sac gland carcinoma. **Veterinary and Comparative Oncology**, v. 15, p. 299–306, 2015

RUBALTELLI, L.; POTRO, E.; SALMASO, R. *et al.* Sonography of abnormal lymph nodes in vitro: correlation of sonographic and histologic findings. **American Journal of Roentgenology**, v. 155, p. 1241- 1244, 1990.

RUPPEL, M. J.; POLLARD, R. E.; WILLCOX, J. L. Ultrasonographic characterization of cervical lymph nodes in healthy dogs. **Veterinary Radiology and Ultrasound**, v. 60, p. 560–566, 2019.

SAAR, L. I.; GETTY, R. Carnivore lymphatic system. In: Getty R (ed): **Sisson and Grossman's anatomy of domestic animals**, 5th ed. Phil- adelphia: W. B. Saunders Company, 1975;1652–1670.

SILVA, P.; USCATEGUI, R. A. R.; MARONEZI, M. C. *et al*. Ultrasonography for lymph node metastasis identification in bitches with mammary neoplasms. **Scientific Reports**, v. 8, p. 17708, 2018.

SILVER, T. I.; LAWSON, J. A.; MAYER, M. N. Sonographic characteristics of presumptively normal main axillary and superficial cervical lymph nodes in dogs. **American Journal of Veterinary Research**, v. 73, p. 1200-1206, 2012.

STAHLE, J. A.; LARSON, M. M.; ROSSMEISL, J. H. *et al*. Diffusion-weighted magnetic resonance imaging is a feasible method for characterizing regional lymph nodes in canine patients with head and neck disease. **Veterinary Radiology and Ultrasound**, v. 60, p. 176–183, 2019.

STAN, F.; GUDEA, A.; DAMIAN, A. *et al*. Ultrasonographic Algorithm for the Assessment of Sentinel Lymph Nodes That Drain the Mammary Carcinomas in Female Dogs. **Animals**, v. 10, p. 2366, 2020.

SUN, F.; BAEZ-DIAZ, C.; SANCHEZ-MARGALLO, F. M. Canine prostate models in preclinical studies of minimally invasive interventions: part I, canine prostate anatomy and prostate cancer models. **Translational Andrology and Urology**, v. 6, p. 538-546, 2017.

WAINBERG, S. H.; OBLAK, M. L.; GIUFFRIDA, M. A. Ventral cervical versus bilateral lateral approach for the extirpation of mandibular and medial retropharyngeal lymph nodes in dogs. **Veterinary Surgery**, v. 47, p. 629-633, 2018.

YING, M.; AHUJA, A.; BROOK, F. *et al*. Vascularity and grey-scale sonographic features of normal cervical lymph nodes: variations with nodal size. **Clinical Radiology**, v. 56, p. 416-419, 2001.

4 COMPUTED TOMOGRAPHIC CHARACTERISTICS OF NORMAL, REACTIVE, AND NEOPLASTIC LYMPH NODES IN DOGS: A SYSTEMATIC REVIEW

ABSTRACT

Computed tomography is routinely used to investigate metastatic lymph nodes and for tumoral staging. The detection of neoplastic or metastatic lymph nodes determines the treatment choices, prognostics and survival time. For that reason, the classification of benign and malignant etiologies must be accurate. A wide range of tomographic features can be used to classify benign and malignant lymph nodes. However, there is an overlap between the classification of reactive and neoplastic or metastatic lymph nodes, so one must rely on cytology or histopathology to confirm the diagnosis. This systematic review presents a qualitative synthesis of studies with description of tomographic features of canine lymph nodes associated with metastatic or inflammatory processes. It aims to provide evidence and elements to enable a more accurate classification of lymphadenopathies in dogs based on computed tomographic investigations. Data was retrieved from PubMed, SCOPUS and Web of Science. Eligibility criteria were studies with lymph nodes; in the canine species; with objective or subjective tomographic description of lymph nodes; in the Portuguese, English or Spanish language. That was extracted information about tomographic dimensions, and pre- and post-contrast attenuation of the lymph nodes or subjective description of tomographic features to differentiate benign and malignant lymphadenopathy. We identified 37 studies (from 2317 database records) that met the inclusion criteria. From that, 9 studies presented tomographic features of normal lymph nodes, 20 of lymphadenopathy associated with neoplasia or metastasis and 8 described lymphadenopathies associated with infectious and/or inflammatory processes. From those studies, 10 provided dimensions of normal lymph nodes, 6 described normal values for pre- and post-contrast attenuation, 8 described attenuation values of lymphadenopathies of any cause, and 13 studies provided a subjective description of lymph nodes on CT exams. Homogeneous enhancement pattern, regular margins and preserved size are some features associated with normal lymph nodes. However the distinction of the different causes of lymphadenopathy remains somehow controversial. For that reason, there is evidence of methods used to improve the accuracy of the tomographic differentiation of the lymphadenopathies. Those included the association of parameters such as size, enhancement pattern, and aspect of the perinodal fat. In this way, we confirm our hypothesis that the tomography provides important information regarding the nodal status aiding the diagnosis of lymphadenopathies of benign or malignant origin.

Keywords: Lymph node. Dog. Computed Tomography. Reactive. Metastatic. Neoplastic. Lymphadenopathy.

4.1 INTRODUCTION

Computed tomography is routinely used to investigate metastatic lymph nodes and for tumoral staging The detection of neoplastic or metastatic lymph nodes determines the treatment choices, prognostics and survival time. For that reason, the

classification of benign and malignant etiologies must be accurate. A wide range of tomographic features can be used to classify benign and malignant lymph nodes. Some authors suggest that a combination of characteristics such as size, attenuation and aspect of perinodal fat, increases the accuracy of the classification. However, there is an overlap between the classification of reactive and neoplastic or metastatic lymph nodes, so one must rely on cytology or histopathology to confirm the diagnosis. Therefore, a clear tomographic distinction between normal, reactive and neoplastic lymph nodes has not yet been established. In this way, this systematic review aims to provide evidence and elements to enable a more accurate classification of lymphadenopathies based on computed tomographic investigations. Our hypothesis is that tomography can differentiate between normal, reactive, and neoplastic (metastatic or primary neoplasia) lymph nodes in dogs.

4.2 MATERIAL AND METHODS

4.2.1. Terminology

This initial description of terms is important to standardize the systematic approach providing a clear definition of each term, according to the MeSH database from NCBI. Lymphadenopathy was described as "a disease of lymph nodes which are abnormal in size, number or consistency". We clarify that it can be related to neoplastic/metastatic or non-neoplastic/metastatic factors. Lymph node metastasis is "the transfer of a neoplasm from its primary site to the lymph node or distant part of the body by way of the lymphatic system". Reactive lymphoid hyperplasia is "a benign infiltration of lymphoid cells or histiocytes". Additionally, reactive lymph nodes may be draining inflammatory reactions secondary to neoplasia or infection. And therefore may present different cellular types according to the origin of the inflammation.

4.2.2. Systematic review and inclusion criteria

This study followed the PRISMA statement (Preferred Reporting Items for Systematic Reviews and Meta-analysis) (MOHER et al., 2009). Literature review was

conducted using PubMed, SCOPUS and Web of Science databases on April 13th 2022 and August 4th 2022. We used the following combinations of terms as descriptors: “reactive lymph node” AND ”tomography" AND "dog"; “neoplastic lymph node” AND ”tomography” AND "dog"; “metastatic lymph node” AND ”tomography” AND ”dog"; “inflammatory lymph node” AND ”tomography” AND ”dog”; “lymph node” AND "tomography". Our search used the filter by subject area in SCOPUS (veterinary and agricultural and biological science), filter by categories in Web of Science (medicine experimental research, veterinary sciences, biology, anatomy morphology, zoology and agriculture and dairy animal science), and filter by species (other animals) on PUBMED. A total of 1063 results were obtained in PubMed, 506 studies in SCOPUS and 748 studies in the Web of Science database.

Studies identified were screened by title, abstract, or both, and duplicates were removed. 76 full-articles were assessed for eligibility (25 from PubMed, 51 from SCOPUS and 54 from Web of Science). The eligible articles were obtained via Periodicos CAPES electronic library. We used the Mendeley software for reference management. To be included in this research, a study had to: 1. Involve tomographic exams of canine lymph nodes; 2. present objective or subjective tomographic description of lymph nodes; 3. be written in Portuguese, English or Spanish language. Exclusion criteria used for screening contemplated studies with lymphography; sentinel lymph node mapping; different animal species (other than dog) or humans; different imaging modalities (other than tomography); description of surgical protocols, clinical treatment, radiation or chemotherapy protocols; anatomic descriptions, and post-mortem studies.

4.2.3. Data extraction

37 full-articles were included in the systematic review. The selection process (PRISMA diagram) is shown in Figure 1. For each study, that was recorded the first author’s name, year, and name of the publication, study groups, sample size, cytological or histopathological results, and healthy status of animal and lymph nodes. We also extracted mean value for length, height and width of lymph nodes (when available), mean pre- and post-contrast attenuation values, and qualitative tomographic characteristics such as homogeneity of the parenchyma, margination

and hilum definition. Information about anatomical location or number of lymph nodes detected at each location were not retrieved. The full dataset of studies was listed in boxes 1, 2 and 3.

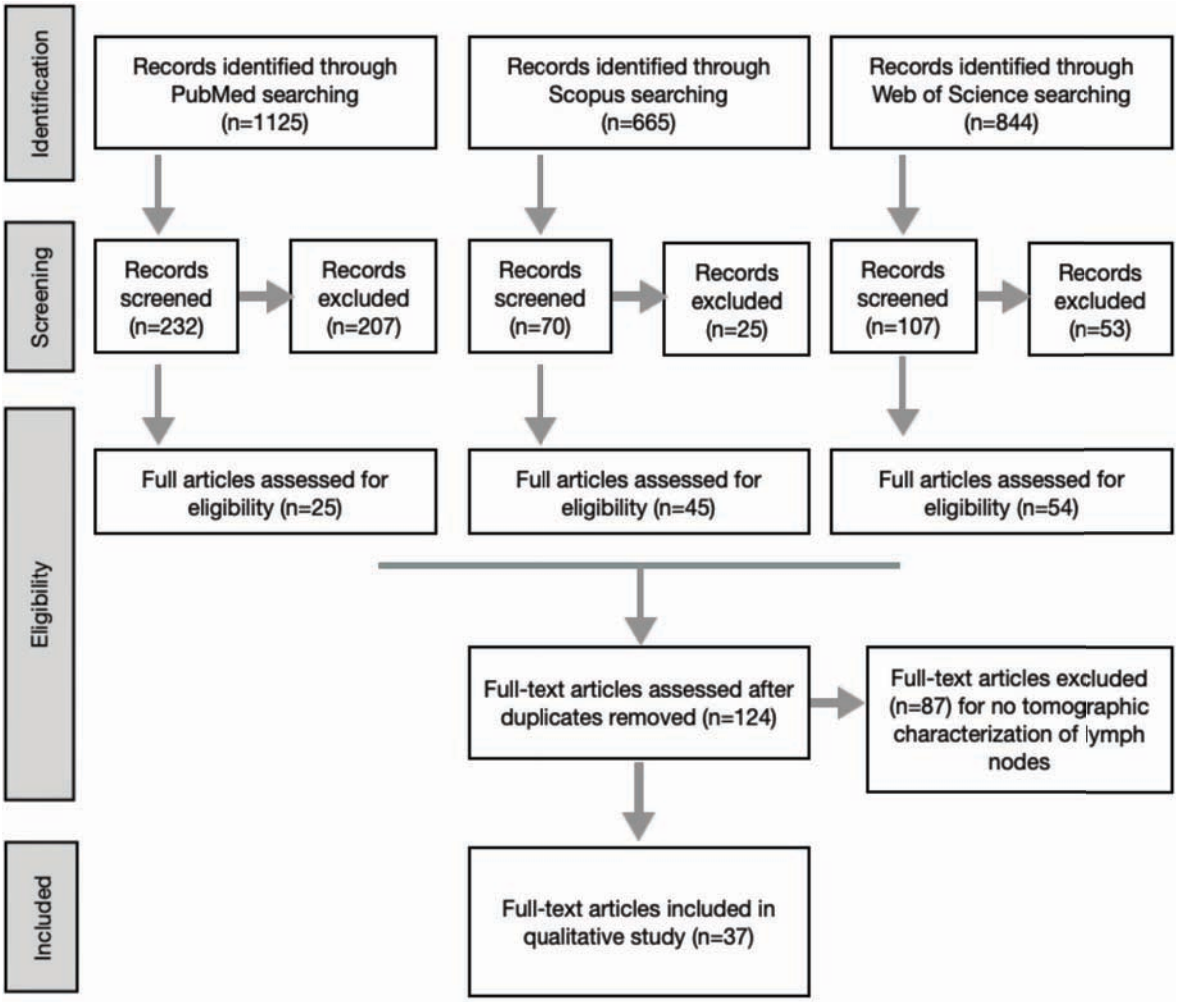

Figure 1: PRISMA flow diagram of literature search and study selection process.

Box 1. Studies with computed tomography of normal lymph nodes in dogs

Sample Size	Lymph node	Study type	Reference
161 dogs with presumed normal lymph nodes	Mandibular and medial retropharyngeal	RET	BELOTTA et al., 2022
100 dogs with normal thorax	Sternal, cranial mediastinal, tracheobronchial, aortic thoracic and pulmonary	RET	KAYANUMA el al., 2020
15 clinically healthy rottweiler dogs	Mediastinal and axillary	PRO	PINTO et al, 2013
102 CT scans with normal canine cervical lymph nodes	Mandibular and medial retropharyngeal	RET	KNEISSLL; PROBST, 2007
19 healthy dogs	Jejunal, splenic, gastric, pancreaticoduodenal, lumbar, renal, medial iliac, internal iliac, sacral, colic and caudal mesenteric, ileocolic	RET	BEUKERS; GROSSO; VOORHOUT, 2013
152 dogs with presumed normal sternal lymph nodes	Sternal	RET	IWASAKI et al., 2016
12 clinically healthy dogs	Sternal	PRO	MILOVANCEV; NEMANIC; BOBE, 2017
27 clinically healthy dogs	Sternal	PRO	STEHLIK et al., 2020
45 clinically healthy	Jejunal, medial iliac, gastric, hepatic, duodenal, pancreatic, splenic, jejunal	RET	TEODORI et al., 2021

Abbreviations: RET: retrospective; PRO: prospective; CT: computed tomography.

Box 2. Studies with computed tomography of malignant lymphadenopathies in dogs			
Sample Size	**Lymph node**	**Study type**	**Reference**
36 dogs with metastasis and 21 control group	Sternal	RET-C	IWASAKI et al., 2018
14 dog with oral melanoma	Medial retropharyngeal, mandibular	RET, OA	COTTER et al., 2021
18 dogs with lymphadenopathy and 10 control group	Tracheobronchial	RET	BALLEGEER el al., 2010
12 dogs with ASGC	Medial iliac, internal iliac	PRO	POLLARD, FULLER; STEFFEY, 2015
30 presumed healthy dogs and 20 with AGASAC	Medial iliac	COS	PALLADINO et al., 2016
16 dogs with gastric tumor	Gastric, hepatic, splenic, pancreaticoduodenal, jejunal, sternal	RET-CS	TANAKA et al., 2019
1 dog with retroperitoneal gastrointestinal stromal tumor	Inguinal	CR	ZHOUG et al., 2017
14 dogs with tonsillar neoplasia	Mandibular and medial retropharyngeal	RET-CS	THIERRY et al., 2018
20 dogs with malignant and 8 with benign oral masses	Medial retropharyngeal and mandibular	RET-M	LEE et al, 2021
1 dog with mediastinal fibrosarcoma	Sternal	CR	MCGRATH et al., 2022
1 dog with AGASAC	Lumbo-aortic, medial and internal iliac	CR	KENNY et al., 2020
4 dogs with primary nodal hemangiosarcoma	Mandibular, retropharyngeal and cranial mediastinal	CS	CHAN et al., 2016
25 with pharyngeal neoplasia	Medial retropharyngeal and mandibular	RET-C	CAROZZI et al, 2015
1 dog with hepatic tumor	Hepatic	CR	KUTARA et al., 2017
2 dogs with abscessation secondary to neoplasia	Medial retropharyngeal	CR	CLOSE et al., 2022
40 oral and nasal tumor	Mandibular and medial retropharyngeal	RET-DA	SKINNER et al., 2018
33 dogs with mammary gland tumor	Superficial inguinal	RET-CC	SOULTANI et al., 2021
16 dogs with neoplasia	Cervical, abdominal, sternal	RET	BONAPARTE et al., 2016
24 dogs oral malignant melanoma	Mandibular	RET	CHOISUNIRACHON et al., 2014
12 dogs with multicentric lymphoma	Neck, thoracic and pelvic limbs, iliosacral, thorax, abdomen, cranial and caudal mesenteric	RET	JONES et al., 2017

Abbreviations: RET-C: retrospective cross-sectional; RET-OA: retrospective, observer agreement; RET: retrospective; PRO: prospective; COS: cohort study; RET-CS: retrospective case series; CR: case report; RET-M: retrospective multicentric; CS: case series; RET-DA: retrospective diagnostic accuracy; RET-CC: retrospective case control; ASGC: anal sac gland carcinoma; AGASAC: apocrine gland anal sac adenocarcinoma; SCC: squamous cell carcinoma.

Box 3. Studies with computed tomography of benign lymphadenopathies in dogs

Sample Size	Lymph node	Study type	Reference
6 dogs with *Angiostrongylus vasorum*	Tracheobronchial, sternal and mediastinal	EXR	DENLER et al., 2010
1 dog with *Coccidioides posadasii* with cervical dissemination	Mandibular and medial retropharyngeal	CR	IZQUIERDO et al., 2020
1 dog with truncal cutaneous pythiosis	Medial iliac	CR	THIEMAN et al., 2011
30 dogs with normal prostate, prostatitis or benign prostatic hyperplasia	Internal iliac	PRO	VALI et al., 2019
1 dog with Leishmaniasis	Popliteal and medial iliac	CR	KONIG et al., 2019
7 dogs with masticatory myositis	Parotid, mandibular, lateral and medial retropharyngeal	RET-CS	REITER; SCHWARZ, 2007
35 dogs and 5 cats with grass awn with intrathoracic migration	Tracheobronchial, cranial mediastinal	RET	SCHULTZ; ZWINGENBERGER, 2008
1 cryptorchid dog	Medial iliac	CR	STOKOWISH et al., 2016

Abbreviations: EXR: experimental research; CR: case report; PRO: prospective; RET-CS: retrospective case series; RET: retrospective.

4.3 RESULTS

From the 37 studies included, 9 were descriptions of CT exams of normal lymph nodes in dogs (Box 1). Those research papers included 3 prospective and 6 retrospective studies. From those, 2 described lymph nodes of the head and neck, 5 studies described lymph nodes of the thorax or thoracic limbs, and 2 described abdominal, iliosacral or pelvic limb lymph nodes.

28 studies described CT exams of abnormal lymph nodes and were separated in malignant (20/28) (Box 2) and benign etiologies (8/28) (Box 3). From the 20 studies describing neoplastic/metastatic lymph nodes, 5 were case reports, 4 were retrospective studies, retrospective-cross-sectional and retrospective-case series accounted for 2 studies each. Retrospective-observer agreement, prospective, Cohort study, retrospective-multicentric, case series, retrospective-diagnostic accuracy and retrospective-case control accounted for one study each. From those, 10 studies included lymph nodes of the head and neck, 6 described lymph nodes of the thorax and thoracic limbs, and 9 described abdominal, iliosacral and lymph nodes from the pelvic limbs.

From the 8 studies presenting benign lymphadenopathies, 4 were case reports, and the others were experimental research, prospective, retrospective, and retrospective-case series (with 1 study each). From those, 2 described lymph nodes from the head and neck, 2 of the thorax or thoracic limbs, and 4 described abdominal, iliosacral or pelvic limb lymph nodes.

Most of the studies included in this systematic review were published in the past decade (30/37) with a uniform distribution within the past five (15/37) and ten years (15/37). Our data collection did not use the filter by year of publication.

Dimensions and pre- and post contrast attenuation values for normal lymph nodes were presented in Boxes 4 and 5. Attenuation values reported for neoplastic, metastatic and reactive lymph nodes in dogs and were presented in Box 6. Some researches provided values for the dimensions of metastatic lymph nodes such as mandibular and medial retropharyngeal lymph nodes with metastasis of oral melanoma (COTTER et al., 2021), inguinal lymph node with metastasis of retroperitoneal gastrointestinal stromal tumor (ZHOUG et al., 2017), and abdominal and sternal lymph nodes with metastasis from gastric lymphoma and adenocarcinoma (TANAKA et al., 2018). However, we decided not to mention those specific measurements based on the fact that one should associate size to other tomographic parameters in order to better diagnose lymphadenopathies, as it will be reinforced by evidence of literature as follows.

BOX 4. Dimensions of lymph nodes from head and neck, thorax and abdomen of healthy dogs

Lymph node	Dimension	N	Reference
Mandibular and medial retropharyngeal	Mandibular lymph node with 0,1-0,25cm length. Medial retropharyngeal lymph node with 0,3-0,7cm length 0,1cm height 0,05-0,1cm width	102	KNEISSL; PROBST, 2007
Mandibular and medial retropharyngeal	Median short axis transverse diameter of 0,52cm for mandibular and 0,54cm for medial retropharyngeal lymph node	161	BELOTTA et al., 2022
Thoracic	Mean long x short axis length for sternal lymph nodes 0,51x0,31cm; cranial mediastinal 0,45x0,31cm; middle tracheobronchial 0,87x0,30cm; intercostal 0,51x0,21cm	100	KANAYUMA et al., 2020
Sternal	Median length x height x width of 0,85x0,60x0,50cm	12	MILOVANCEV; NEMANIC; BOBE, 2017
Mediastinal and axillary	Short axis diameter average 0,35cm for the axillary lymph node and 0,47cm for the mediastinal lymph node	15	PINTO et al., 2013
Sternal	Mean long axis 0,70cm. Mean short axis 0,36cm. Ratio short axis:height of the second sternebra 0,457	152	IWASAKI et al., 2016
Medial iliac	Lymph node:aorta ratio ≥1.3	30	PALLADINO et al., 2016
Iliosacral	Length x width x height was 2,28x0,67x0,46cm for the medial iliac and 1,03x0,48x0,37cm for internal iliac and sacral lymph nodes	19	BEUKERS; GROSSO; VOORHOUT, 2013
Abdominal	Length x width x height was 1,61x0,67x0,52cm for hepatic; 1,07x0,57x0,44cm for splenic; 0,87x0,72x0,53cm for gastric; 0,78x0,59x0,44cm for pancreaticoduodenal; 0,92x0,45x0,31cm for lumbar aortic; 0,88x0,53x0,31cm for renal; 4,2x0,96x0,71cm for jejunal; 0,97x0,61x0,49cm for ileocolic; and 0,88x0,61x0,45cm for caudal mesenteric lymph nodes	19	BEUKERS; GROSSO; VOORHOUT, 2013
Abdominal and iliosacral	Median length x height x width was 1,94x0,49x0,53cm for hepatic; 1,47x0,45x0,51cm for splenic; 0,96x0,51x0,57cm for gastric; 0,91x0,58x0,44cm for pancreaticoduodenal; 2,46x0,52x0,49cm for medial iliac; and 0,50x0,58x0,65cm for jejunal lymph nodes	45	TEODORI et al., 2021

BOX 5. Attenuation pré- and post-contrast of lymph nodes from head and neck, thorax and abdomen of healthy dogs

Lymph node	Attenuation pré-contrast (HU)	Attenuation post-contrast (HU)	N	Reference
Mandibular and medial retropharyngeal	Median attenuation 32,3HU for the mandibular and 31,8HU for the medial retropharyngeal	-	161	BELOTTA et al., 2022
Medial retropharyngeal	45HU	114.6HU	102	KNEISSL; PROBST, 2007
Cervical and abdominal	Cervical with 36.6 HU Abdominal mean 37HU	Cervical with mean 110,3HU. Abdominal with mean 109HU	19	BEUKERS; GROSSO; VOORHOUT, 2013
Abdominal and iliosacral	Median 29HU for hepatic; 29,5HU for splenic; 24HU for gastric; 27HU for pancreaticoduodenal; 27HU for medial iliac, and 28HU for jejunal lymph nodes	Median 94HU for hepatic; 91.5HU for splenic; 89.5HU for gastric; 90HU for pancreaticoduodenal; 89.5HU for medial iliac; and 98HU for jejunal lymph nodes	45	TEODORI et al., 2021
Sternal	Median 18.3HU	Median 41.3HU	12	MILOVANCEV; NEMANIC; BOBE, 2017
Sternal	Mean 30.2HU and median 29HU	Mean 61.7HU and median 62HU	152	IWASAKI et al., 2016

HU: Hounsfield units

BOX 6. Attenuation pré- and post-contrast of metastatic, neoplastic or reactive lymph nodes from head and neck, thorax and abdomen of dogs

Lymph node	Attenuation pré-contrast (HU)	Attenuation post-contrast (HU)	Sample size and etiology	Reference
Mandibular	Mandibular with 34.7HU and medial retropharyngeal with 34,9HU	Mandibular with 96.4HU and medial retropharyngeal with 102,6HU	40 dogs with oral and nasal cancer	SKINNER et al., 2018
Tracheobronchial	Mean 43.9HU before treatment	Mean 87.3HU before treatment	6 dogs with *Angiostrongylus vasorum*	DENLER et al., 2010
Mediastinal	Mean 41.6HU before treatment	Mean 81.2HU before treatment	6 dogs with *Angiostrongylus vasorum*	DENLER et al., 2010
Superficial inguinal	Periphery of metastatic lymph nodes with 42.05HU and center with 41.8HU	Periphery of metastatic lymph nodes with 61.95HU and center with 60.45HU. Densities higher than 74.1HU on the periphery and 90HU in the center are highly suggestive of metastasis	33 dogs with mammary gland tumor	SOULTANI et al., 2021
Mandibular amd medial retropharyngeal	Median 36HU	Median 92HU	14 dogs with tonsillar neoplasia	THIERRY et al., 2018
Abdominal	Mean 42.9HU of enlarged lymph nodes for lymphoma cases	Mean 73.8HU of enlarged lymph nodes for lymphoma cases	16 dogs with gastric tumor	TANAKA et al., 2019
Abdominal	Mean 36.9HU of enlarged lymph nodes for adenocarcinoma cases	Mean 61.1HU of enlarged lymph nodes for adenocarcinoma cases	16 dogs with gastric tumor	TANAKA et al., 2019
Sternal	Median 41.1HU	Median 76.1HU	36 with metastasis	TANAKA et al., 2019

HU: Hounsfield units

4.4 DISCUSSION

The cross-sectional evaluation of lymph nodes may be challenging due to their small size and intimate proximity to other soft tissue structures. The thickness of the tomographic slices is one of the factors influencing the detection of small lymph nodes. Thicker the slice, higher the chances of missing some tiny structures during the investigation. This effect, called partial volume artifact, can also be the cause of

lower pre-contrast density of presumed normal canine sternal lymph nodes (11.7 HU) (STEHLIK et al., 2020).

Perinodal fat was seen in all dogs evaluated, and favored the distinction of the sternal lymph nodes from the surrounding cranial mediastinal structures (MILOVANCEV; NEMANIC; BOBE, 2017). Similar considerations were made for abdominal and iliosacral lymph nodes. Their tomographic detection and differentiation from the adjacent soft tissue structures was improved by intra-abdominal fat (BEUKERS; GROSSO; VOORHOUT, 2013).

The size of the lymph nodes vary according to each lymph node type, and the size alone is not a reliable malignancy marker (WILLIAMS; PARKER, 2003; IWASAKI et al., 2017). For that reason, it is important to consider other features, such as the enhancement pattern (BALLAGEER et al., 2010), or the association between size and pre-contrast attenuation (IWASAKI, 2018). The combination between marked enlargement, rounded shape and heterogeneous enhancement pattern would prompt a malignant node in 75% of the cases (CAROZZI et al., 2015).

When compared to benign tumors, malignant lymph nodes tend to be enlarged (LEE et al., 2021). Hepatic lymph nodes in a dog with hepatic tumor were enlarged with an heterogeneous contrast pattern with rich marginal enhancement and poor central contrast enhancement (KUTARA et al., 2017).

Enlarged cervical lymph nodes presenting a primary nodal hemangiosarcoma may be associated to a soft tissue attenuating mass with irregular shape and rounded contours displacing trachea and larynx, salivary gland and thyroid, and carotid. It may also be found as a heterogeneous, hypoattenuating contrast-enhancing soft tissue enlarged mass (CHAN et al., 2016).

Mandibular lymph nodes presenting metastasis of oral melanoma were slightly larger than non-metastatic lymph nodes. This can be related to the infiltration of turmoil cells or local inflammation secondary to the neoplasia (CHOISUNIRACHON et al., 2014). Other studies with oral melanoma suggested the importance of cytology or histopathology regardless of the nodal size to ensure an accurate staging (WILLIAMS; PARKER, 2003).

Linfonodomegaly is very commonly identified on CT and can be regional or widespread according to the tumor type (BONAPARTE et al., 2016). A study with gastric tumors revealed that adenocarcinoma showed regional lymphadenopathy,

while gastric lymphoma presented disseminated lymphadenopathy (TANAKA et al., 2019). Medial retropharyngeal lymph nodes were more frequently affected in pharyngeal neoplasia (CAROZZI et al., 2015) and tonsillar neoplasia (THIERRY et al., 2018) in dogs, when compared to mandibular lymph nodes.

Some normal abdominal lymph nodes in dogs presented a rounded shape with a short axis/long axis ratio >0.5 (BEUKERS; GROSSO; VOORHOUT, 2013). Conversely, the rounded shape of regional lymph nodes (short axis/long axis ratio >0.47) was associated with malignancy in a study with gastric tumors in dogs. All lymphomas and adenocarcinomas presented enlarged, round-shaped regional abdominal lymph nodes (TANAKA et al., 2019).

The shape of the lymph nodes is directly affected by tumoral infiltration that leads to expansion of the capsule. The rounded (LEE et al., 2021) or irregular shape can suggest metastatic infiltration on CT (STOKOWSKI et al., 2016).

All presumed normal canine sternal lymph nodes presented a defined fat-attenuating or hypoattenuating hilus (MILOVANCEV; NEMANIC; BOBE, 2017). Enlarged retropharyngeal lymph nodes associated with tonsillar neoplasia in dogs were related to loss of the nodal hilus in 91% of the cases (THIERRY et al., 2018). Regarding to nodal heterogeneity, a heterogeneous parenchyma with hypoattenuating center on post-contrast images (associated with necrosis) (THIERRY et al., 2018) or hypoattenuating foci resembling cystic changes (LEE et al., 2021) are associated with malignancy.

Another computed tomographic parameter to identify healthy and abnormal structures is the quantification of the attenuation coefficient or Hounsfield unit difference between those structures (BONAPARTE et al., 2016).

The attenuation is related to the density of the tissues. Therefore, the tomographic detection of lesioned areas in the parenchyma of different organs depends on their density compared to the density of the adjacent healthy tissue. Nodal parenchymal density in case of neoplastic infiltration may not be distinguished from the aspect of the normal parenchyma (JONES et al., 2017), depending on the tumor type and stage of the disease.

The use of contrast highlight differences in attenuation (i.e. between nodal parenchyma and perinodal fat) and can improve significantly the tomographic exam

aiding in the evaluation of anatomic structures and localization of lesions (POLLARD; FULLER; STEFFEY, 2015; BONAPARTE et al., 2016).

Contrast enhancement pattern facilitates the characterization of solid lesions as hypo or hypervascular masses (BONAPARTE et al., 2016). Lymph nodes present an evident vascularization and, therefore, high contrast enhancement. Their post-contrast attenuation will differ from that of the pre-contrast series enabling the detection of tissue abnormalities such as metastatic foci or tumor cell infiltration (STEHLIK et al., 2020). The characterization of benign and aggressive disease may be related to the fact that circulation disruption caused by tumor infiltrates prompts abnormal enhancement patterns (NYMAN et al, 2005). contrast enhanced CT of the pelvis was superior to ultrasound to detect iliosacral lymph noes in dogs with anal sac gland tumors (POLLARD; FULLER; STEFFEY, 2015).

Attenuation values lower than normal in the pre-contrast series can be related to the partial volume artifact (as most of the nodes present a very small size, the region of interest may sometimes include some perinodal fat and this will diminish the density) (STEHLIK et al., 2020). There could be high HU values in both pre- and post-contrast phases in case of larger lymph nodes and consequently larger regions of interest (ROI).

A study with normal sternal lymph nodes reported that there was a homogeneous enhancement pattern in the pre-contrast phase and a heterogeneous enhancement after contrast administration, revealing a difference in the cortical and medullary regions with a higher attenuation in the periphery of the lymph node (IWASAKI et al., 2016).

Heterogeneous contrast enhancement can produce a ring pattern normally seen with lymphadenomegaly (SKINNER et al., 2018) and can suggest neoplastic infiltration on CT (BALLAGEER et al., 2010; STOKOWSKI et al., 2016). The enhancement pattern, with the nodal periphery more hyperattenuating, can also be related to areas of abscessation, cystic formation, hemorrhage, mineralization or circulation disruptions that follows tumor infiltration (BEUKERS; GROSSO; VOORHOUT, 2013).

A central area of hypoattenuation in the lymph node can represent tumor cells, necrosis secondary to metastasis, lipid metaplasia or abscess (CAROZZI et al., 2015). Canine tracheobronchial lymph nodes with metastatic lymphadenopathy or

severe granulomatous lymphadenitis presented an abnormal contrast enhancement pattern. Therefore, the differentiation between these must be made with biopsy of the primary lesion (BALLAGEER et al., 2010). Similar considerations were stated for medial retropharyngeal lymph nodes of dogs with tonsillar neoplasia. This lymph node presented heterogeneous post-contrast enhancement with a hypoattenuating center (suggesting nodal necrosis) (THIERRY et al., 2018).

Lumbo-aortic and iliac lymph nodes presented enlargement, heterogeneous contrast enhancement and indistinct margins associated with poorly differentiated carcinoma (KENNY et al., 2020).

Most abdominal lymph nodes in dogs had a homogeneous structure pre- and post-contrast (BEUKERS; GROSSO; VOORHOUT, 2013). Same descriptions were provided for sternal lymph nodes, which presented mildly contrast enhancement (MILOVANCEV, NEMANIC, BOBE, 2017).

In benign oral tumors, enlarged mandibular lymph nodes ipsilateral to the acanthomatous ameloblastoma presented a homogeneously enhancing pattern (LEE et al., 2021).

One of the largest intrathoracic lymph nodes identified in a case series study was associated with an enlarged tracheobronchial lymph node with granulomatous lymphadenitis secondary to blastomycosis (BALLAGEER et al., 2010).

Dental problems may also lead to lymphadenopathy (LEE et al, 2021). Interestingly, lymphadenopathy may not be detected in some inflammatory processes. The absence of lymphadenopathy may suggest a benign lesion, such as reported for gastric tumors (inflammatory polyps and leiomyomas) (TANAKA et al., 2019).

A case report of masticatory myositis described enlarged mandibular and medial retropharyngeal lymph nodes, with mild to marked central contrast enhancement, or homogeneous patterns (REITER; SCHWARZ, 2007).

Mildly enlarged popliteal and medial iliac lymph nodes with a moderate, homogeneous contrast enhancement were positive for leishmaniasis on serology (KONIG et al., 2019).

A study described a severely enlarged medial retropharyngeal lymph node with minimal peripheral contrast enhancement and multiple base bubbles. This lymph node was suspected of abscessation and was adjacent to a mass suspected of

tonsillitis or tonsil abscessation. Cytology revealed a reactive lymph node with a septic suppurative inflammatory process and no evidence of neoplastic cells (CLOSE et al, 2022).

Pythiosis is frequently disseminated to regional lymph nodes. A report of truncal cutaneous pythiosis in a dog described enlargement of the medial iliac lymph node and cytology consistent with reactive lymphoid hyperplasia (THIEMAN et al., 2011).

Internal medial iliac lymph node length can be used for differentiating prostatitis from normal prostate and benign prostatic hyperplasia. The pathological exams should be performed as a gold standard to evaluate both prostate and lymph nodes and confirm the diagnosis (VALI et al, 2019).

A sternal lymph node presented mild enlargement and rounded shape in a case report of mediastinal fibrosarcoma. Histopathology of regional lymph nodes and immunolabeling revealed atypical reactive mesothelial cells (MCGRATH et al., 2022).

Mandibular and medial retropharyngeal lymph nodes adjacent to a subcutaneous mass diagnosed as coccidioidomycosis presented heterogeneous central contrast enhancement and a ring-distribution pattern (strong peripheral enhancement). The fat planes between the lymph nodes, left mandibular salivary gland, and muscle bellies were disrupted by the perinodal linear soft tissue striations (IZQUIERDO et al., 2020).

4.5 CONCLUSION

To our knowledge, this systematic review is the first to provide evidence of tomographic characteristics commonly associated with normal, reactive and neoplastic lymph nodes. In general, heterogeneous post-contrast enhancement pattern and irregular or indistinct margins may be associated with malignant etiologies. But the combination tomographic characteristic improve the detection and differentiation of benign and malignant processes. The perinodal fat tissue represents a natural contrasting surface and improves the detection of the lymph node. However, the inclusion of perinodal fat in the region of interest can produce inaccurate attenuation values. The absence of lymphadenopathy associated with a tumoral mass may suggest a benign lesion. Nonetheless cytology or histopathology must be performed to confirm the diagnosis.

ACKNOWLEDGEMENTS

This study was supported by the Coordination for the Improvement of Higher Education Personnel, Brazilian Ministry of Education (CAPES PDSE, process 88887.368578/2019-00) and Sao Paulo Research Foundation (FAPESP, process 2020/04868-9) fellowships to Anna C. M. Ercolin.

REFERENCES

BALLEGER, E. A.; ADAMS, W. M.; DUBIELZIG, R. R. *et al*. Computed tomography characteristics of canine tracheobronchial lymph node metastasis. **Veterinary Radiology and Ultrasound**, v. 51, p. 397–403, 2010.

BELOTTA, A. F.; SUKUT, S.; LOWE, C. *et al*. Computed tomography features of presumed normal mandibular and medial retropharyngeal lymph nodes in dogs. **Canadian Journal of Veterinary Research**, v. 86, p. 27-34, 2022.

BEUKERS, M.; GROSSO, F. V.; VOORHOUT, G. Computed tomographic characteristics of presumed normal canine abdominal lymph nodes. **Veterinary Radiology and Ultrasound**, v. 54, n. 6, p. 610–617, 2013.

BONAPARTE, A.; DHALIWAL, R. S.; HEO, J. *et al*. Whole Body Computed Tomography for Tumor Staging in Dogs: Review of 16 Cases. **Journal of Veterinary Science and Technology**, v.7, n. 4, 2016.

CAROZZI, G.; ZOTTI, A.; ALBERTI, M. *et al*. Computed tomographic features of pharyngeal neoplasia in 25 dogs. **Veterinary Radiology and Ultrasound**, v. 56, n. 6, p. 628–637, 2015.

CHAN, C. M.; ZWAHLEN, C. H.; DE LORIMIER, L. P. *et al*. Primary nodal hemangiosarcoma in four dogs. **Journal of American Veterinary Medical Association,** v. 249, p. 1053–1060, 2016.

CHOISUNIRACHON, N.; LIN, L. S.; TANAKA, Y.; SAEKI, K. *et al*. Characterization of canine oral malignant melanoma in 24 dogs. **Thaiwan Journal of Veterinary Medicine**, v. 44, n. 4, p. 497-503, 2014.

CLOSE, E.; LUMBRAZER-JOHNSON, S.; HOSTNIK, E. *et al*. Lymph node abs cessation secondary to neoplasia in two dogs. **Case Reports in Veterinary Medicine,** 2022.

COTTER, B.; ZWICKER, L. A.; WALDNER, C. *et al*. Inter- and intraobserver agreement for computed tomographic measurement of mandibular and medial retropharyngeal lymph nodes is excellent in dogs with histologically confirmed oral melanoma. **Veterinary Radiology and Ultrasound**, v. 63, p. 73–81, 2022.

DENLER, M.; MAKARA, M.; KRANJC, A. *et al*. Thoracic computed tomography findings in dogs experimentally infected with Angiostrongylus vasorum. **Veterinary Radiology and Ultrasound**, v. 52, n. 3, p. 289-294, 2011.

IWASAKI, R.; MORI, T.; ITO, Y. *et al* Computed tomographic evaluation of presumptively normal canine sternal lymph nodes. **Journal of the American Animal Hospital Association**, v. 52, p. 371–377, 2016.

IWASAKI, R.; MURAKAMI, M.; KAWABE, M. *et al*. Metastatic diagnosis of canine sternal lymph nodes using computed tomography characteristics: A retrospective cross-sectional study. **Veterinary and Comparative Oncology**, p. 1-8, 2017.

IZQUIERDO, A.; JAFFEY, J. A.; SZABO, S. *et al*. *Coccidioides posadasii* in a dog with cervical dissemination complicated by esophageal fistula. **Frontiers in Veterinary Sciences**, v. 7, p. 285, 2020.

JONES, I. D.; DANIELS, A. D.; LARA-GARCIA, A. *et al*. Computed tomographic findings in 12 cases of canine multicentric lymphoma with splenic and hepatic involvement. **Journal of Small Animal Practice,** 2017.

KAYANUMA, H.; YAMADA, K.; MARUO, T. *et al.* Computed tomography of thoracic lymph nodes in 100 dogs with no abnormalities in the dominated area. **The Journal of Veterinary Medical Science**, 2019.

KENNY, D.; LANTZAKI, V.; AYL, R. *et al*. Computed tomography and magnetic resonance imaging findings in a dog with apocrine gland anal sac adenocarcinoma with vertebral canal metastasis. **Veterinary Records: Case Report**, v. 8, p. e001234, 2020.

KNEISSL, S.; PROBST, A. Comparison of computed tomographic images of normal cranial and upper cervical lymph nodes with corresponding E12 plastinated-embedded sections in the dog. **The Veterinary Journal**, v. 174, p. 435–438, 2007.

KONIG, M. L.; HOWARD, J.; SCHMIDHALTER, M. *et al*. Leishmaniasis manifesting as osteomyelitis and monoarthritis in a dog and outcome following treatment with miltefosine and allopurinol. **Veterinary Records: Case Report**, v. 7, p. e000793, 2019.

KUTARA, K.; KONNO, T.; KONDO, H. *et al*. Triple-phase helical computed tomography of an arterial-hepatic shunt in a hepatic tumor in a dog. **Journal of Veterinary Medical Sciences**, v. 79, n. 12, p. 1947-1951, 2017.

LEE, S.; JANG, Y.; LEE, G. *et al*. CT features of malignant and benign oral tumors in 28 dogs. **Veterinary Records: Case Report**, p. 1–8, 2021.

MCGRATH, A. M.; SALYER, S. A.; SEELMANN, A. *et al*. Mediastinal Fibrosarcoma in a Dog–Case Report. **Frontiers in Veterinary Sciences**, v. 9, p. 820956, 2022.

MILOVANCEV, M.; NEMANIC, S.; BOBE, G. Computed tomographic assessment of sternal lymph node dimensions and attenuation in healthy dogs. **American Journal of Veterinary Research,** v. 78, n. 3, 289-294, 2017.

MOHER, D.; LIBERATI, A.; TETZLAFF, J. *et al*. PRISMA. Preferred reporting items for systematic reviews and meta-analyses: the PRISMA Statement. **Annals of Internal Medicine,** v. 151, n. 4, p. 264-270, 2009.

NYMAN, H. T.; KRISTENSEN, A. T.; SKOVGAARD, I. M.*et al*. Characterization of normal and abnormal canine superficial lymph nodes using gray-scale b-mode, color flow mapping, power, and spectral doppler ultra- sonography: a multivariate study. **Veterinary Radiology and Ultrasound, v.** 46, p. 404–410, 2005.

PALLADINO, S.; KEYERLEBER, M. A.; KING, R. G. *et al*. Utility of computed tomography versus abdominal ultrasound examination to identify iliosacral lymphadenomegaly in dogs with apocrine gland adenocarcinoma of the anal sac. **Journal of Veterinary Internal Medicine**, v. 30, p. 1858–1863, 2016.

PINTO, A. C. B. F.; ANELI, E.; PATARA, A. C. *et al.* Computed tomography image of the mediastinal and axillary lymph nodes in clinically sound Rottweilers. Pesquisa Veterinária Brasileira, v. 33, n. 3, p. 405-410, 2013.

POLLARD, R. E.; FULLER, M. C.; STEFFEY, M. A. Ultrasound and computed tomography of the iliosacral lymphatic centre in dogs with anal sac gland carcinoma. **Veterinary and Comparative Oncology**, v. 15, n. 2, p. 299–306, 2015.

REITER, A. M.; SCHWARZ, T. Computed tomographic appearance of masticatory myositis in dogs: 7 cases (1999–2006). **Journal of the American Veterinary Medicine Association**, v. 231, p. 924–93, 2007.

SCHULTZ, R. M.; ZWINGEENBERGER, A. Radiographic, computed tomographic and ultrasonographic findings with migrating intrathoracic grass awns in dogs and cats. **Veterinary Radiology and Ultrasound,** v. 49, n. 3, p 249-255, 2008.

SKINNER, O. T.; BOSTON, S. E.; GIGLIO, R. F. *et al*. Diagnostic accuracy of contrast-enhanced computed tomography for assessment of mandibular and medial retropharyngeal lymph node metastasis in dogs with oral and nasal cancer. **Veterinary and Comparative Oncology**, p. 1–9, 2018.

SMITH, A. J.; SUTTON, D. R.; MAJOR, A. C. CT appearance of presumptively normal intrathoracic lymph nodes in cats. **Journal of Feline Medicine and Surgery,** p. 1–7, 2019.

STEHLIK, L.; VITULOVA, H.; SIMEONI, F. *et al*. Computed tomography measurements of presumptively normal canine sternal lymph nodes. **BMC Veterinary Research**, v. 16, p. 269, 2020.

SOULTANI, C.; PATSIKAS, M. N.; MAYER, M. *et al*. Contrast enhanced computed tomography assessment of superficial inguinal lymph node metastasis in canine mammary gland tumors. **Veterinary Radiology and Ultrasound,** 2021.

STOKOWSKI, S.; RUTH, J.; LANZ, O. *et al*. Computed Tomographic Features in a Case of Bilateral Neoplastic Cryptorchidism with Suspected Torsion in a Dog. **Frontiers in Veterinary Sciences**, v. 3, p. 33, 2016.

TANAKA, T.; AKIYOSHI, H.; MIE, K. et al. Contrast-enhanced computed tomography may be helpful for characterizing and staging canine gastric tumors. **Veterinary Radiology and Ultrasound**, p. 1-12, 2018.

TEODORI, S.; ASTE, G.; TAMBURRO, R. *et al*. Computed Tomography Evaluation of Normal Canine Abdominal Lymph Nodes: Retrospective Study of Size and Morphology According to Body Weight and Age in 45 Dogs. **Veterinary Sciences**, v. 8, p. 44, 2021.

THIEMAN, K. M.; KIRKBY, K. A.; FLYNN-LURIE, A. *et al*. Diagnosis and treatment of truncal cutaneous pythiosis in a dog. **Journal of the American Veterinary Medicine Association**, v. 239, p.1232-1235, 2011.

THIERRY, F.; LONGO, M.; PECCEU, E. *et al*. Computed tomographic appearance of canine tonsillar neoplasia: 14 cases. **Veterinary Radiology and Ultrasound**, p. 1-10, 2017.

VALI, Y.; SOROORI, S.; MOLAZEM, M. *et al*. Comparison of computed tomographic and cytological results in evaluation of normal prostate, prostatitis and benign prostatic hyperplasia in dogs. **Veterinary Research Forum**, v. 10, p. 17-22, 2019.

WILLIAMS, L. E.; PACKER, R. A. Association between lymph node size and metastasis in dogs with oral malignant melanoma: 100 cases (1987-2001). **Journal of the American Veterinary Medicine Association**, v. 222, n. 9, p. 1234-6, 2003.

ZHOUG, Y.; WU, X. D.; SHI, Q. *et al*. retroperitoneal gastrointestinal stromal tumor with inguinal lymph node metastasis. **International Journal of Clinical Experimentation Medicine**, v. 10, n. 9, p. 13935-13937, 2017.

5 CONCLUSION

Considering all the discussion about pros and cons of the different studied modalities (B-mode ultrasonography and computed tomography), and the advantages and disadvantages of each one to detect and differentiate normal, reactive and neoplastic lymph nodes in dogs, we conclude that the association between different imaging criteria is mandatory to ensure a more accurate diagnosis. The ultrasonographic and tomographic imaging exams are based in anatomo-

morphologic characteristics and were able to provide some interesting information based on the combinations of "margination and perinodal fat" for CT and "size and echotexture" for US.

Cytological or histopathological exams are the gold standard methods as they provide an evaluation at the cellular level. Those tests are important to avoid possible misclassification in cases when there is an overlap among the different lymph node status (based on imaging exams).

APPENDIX 1

Ultrasonographic exams in dogs for the control group

B-mode ultrasound images of cranial cervical, superficial inguinal, and medial iliac lymph nodes of ten healthy dogs were obtained and were randomly allocated between the aforementioned images of abnormal lymph nodes. This prospective part of the study was approved by the Ethical Committee for Animal Experimentation (CEUA) of FZEA USP under the protocol number: 9135150620.

Animals were recruited in the city of Pirassununga, Sao Paulo, Brazil and evaluated at the veterinary hospital UDCH from FZEA USP. The dogs were submitted to clinical examination of the head and neck (with specific attention to the oral cavity and ears), abdomen, and pelvic limbs. Temperature and body weight were recorded. Animals with a history of diseases or any abnormalities found in the clinical exam were excluded from the study.

For the ultrasonographic exams, dogs were physically restrained. The dogs were positioned in dorsal recumbency with the head, neck and limbs extended and had the hair clipped over the cervical and abdominal areas. There were used micro-convex and linear electronic transducers with frequencies based on the depth of the structures evaluated. Measurements were performed in longitudinal and transverse views to estimate the dimension and short-to-long axis ratio for each lymph node.

The exams were performed with a MyLabClass C Vet ultrasound device from Esaote (Esaote, Venice, Italy), with a micro-convex and multi-frequency electronic transducer, varying from 3 to 18 MHz; a linear electronic transducer with frequency ranging from 6,0 a 18,0MHz; and a linear electronic transducer with frequency ranging from 8,0 a 13,0MHz.

Superficial inguinal lymph nodes are more superficial structures located in the subcutaneous layers in the inguinal region. They were better evaluated with the dogs positioned in dorsal recumbency at both sides of the medial region of the inguinal area. Linear transducers with higher frequencies were most frequently preferred for this evaluation (Figure 4A).

Mandibular lymph nodes are very superficial structures and can be found ventrally to the angle of the mandible. They are cranial and lateral to the mandibular salivary gland from each side (Fig. 4B).

Medial iliac lymph nodes were assessed via flank with the animals in lateral recumbency. The anatomical landmark was the region where the caudal aorta originates the external iliacs and circumflex arteries. This lymph node has a deeper location and therefore was better evaluated with the micro-convex transducer, most of the time (Fig. 4C).

Medial retropharyngeal lymph nodes are dorsal to the pharynx and caudomedial to the mandibular salivary gland (Fig. 4D) (PENNINCK; D'ANJOU).

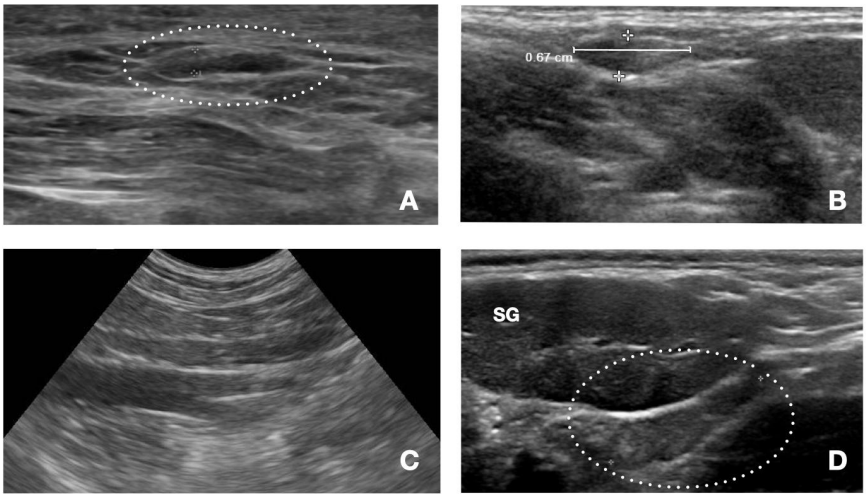

Figure 4: B-mode ultrasonographic images of normal lymph nodes in dogs in longitudinal view. A. Superficial inguinal lymph node with 0,12cm height. B. Mandibular lymph node with 0,67cm x 0,24cm. C. Medial iliac lymph node adjacent to the abdominal aorta at its ramification in the extern iliac and circunflex arteries. D. Medial retropharyngeal lymph node adjacent to the mandibular salivary gland (SG), with 1,51cm length.

APPENDIX 2

ERCOLIN, A.C.M. **Linfonodos.** In: KANAYAMA, L. Atlas de ultrassonografia em cães e gatos. São Paulo: Editora Payá. 2022.

The book chapter about canine lymph nodes, written by Anna Carolina Mazeto Ercolin, is placed in Section 2: Abdominal ultrasonography of the book Atlas de Ultrassonografia em Cães e Gatos, authored by Luciane M. Kanayama (which is still being edited by Payá ed.: Sao Paulo/SP).

First, there is a detailed anatomic description of the lymphocenters and their main lymph nodes at the head and neck, thoracic and pelvic limbs, thorax, abdominal and pelvic wall and abdomen in dogs. There is also a description of the lymphatic territories of each main lymph node at the different regions of the body.

The topographic anatomy of abdominal and iliosacral lymph nodes is presented, highlighting the abdominal vascularization which is closely related to the lymphatic drainage. Anatomical landmarks associated with the gastric, splenic, hepatic, renal, medial iliac, hypogastric, sacral and lumbar aortic lymph nodes are described.

The next topic is about ultrasonographic aspects of normal lymph nodes. It describes the hilum, capsule and nodal parenchyma as well as normal B-mode ultrasonographic parameters (i.e. shape, echogenicity and size) for each specific lymph node, according to literature. There is also a protocol for the ultrasonographic qualitative and quantitative evaluations of lymph nodes including the position of the dogs, types of transducers and scanning techniques to investigate abdominal and iliosacral lymph nodes.

Following there are ultrasonographic characteristics of abnormal lymph nodes and evidence associated with benign (inflammatory or infectious) or malignant processes (neoplastic or metastatic). B-mode ultrasonographic parameters described include hilum definition, size, shape, margination, echogenicity and echotexture. It highlights the importance of the combination of parameters such as margination and perinodal fat or ratio between lymph node height and aortic diameter, since they improve the differentiation of benign and malignant lymphadenopathies.

At last, there is a description of Doppler ultrasonography and its importance to the investigation of different etiologies associated with lymphadenopathy. It includes description of qualitative and quantitative analysis (resistivity and pulsatility index).

This book chapter presents tables, figures, schemes, infographics and short videos of each abdominal and iliosacral lymph node in dogs.